Prolactin-mediates a lactation-induced suppression of arcuate kisspeptin neuronal activity necessary for lactational infertility in mice

Eleni C.R. Hackwell[1,2], Sharon R. Ladyman[1,2,4], Jenny Clarkson[1,3], H. James McQuillan[1,2], Ulrich Boehm[5], Allan E. Herbison[6], Rosemary S.E. Brown[1,3], David R. Grattan[1,2,4]

[1]Centre for Neuroendocrinology, [2]Department of Anatomy and [3]Department of Physiology, School of Biomedical Sciences, University of Otago, Dunedin, NZ; [4]Maurice Wilkins Centre for Molecular Biodiscovery, Auckland, NZ; [5]Saarland University School of Medicine, Centre for Molecular Signalling (PZMS), Experimental Pharmacology, Homburg, Germany; [6]Department of Physiology, Development and Neuroscience, University of Cambridge, Cambridge, United Kingdom.

Corresponding author: David R. Grattan

Email: dave.grattan@otago.ac.nz

Author Contributions:

ECRH: Designed research, completed research, analysed data, wrote the first draft of the manuscript, edited the manuscript.
SRL: Designed research, completed research, analysed data, edited the manuscript.
JC: Completed research, analysed data, edited the manuscript.
HJM: Completed research, edited the manuscript.
UB: Provided key resources, edited the manuscript.
AEH: Designed research, analysed data, edited the manuscript.
RSEB: Designed research, analysed data, edited the manuscript.
DRG: Designed research, provided key resources, analysed data, edited the manuscript.

Competing Interest Statement: The authors have no competing interests to declare.

Abstract

The specific role that prolactin plays in lactational infertility, as distinct from other suckling or metabolic cues, remains unresolved. Here, deletion of the prolactin receptor (Prlr) from forebrain neurons or arcuate kisspeptin neurons resulted in failure to maintain normal lactation-induced suppression of estrous cycles. Kisspeptin immunoreactivity and pulsatile LH secretion were increased in these mice, even in the presence of ongoing suckling stimulation and lactation. GCaMP6 fibre photometry of arcuate kisspeptin neurons revealed that the normal episodic activity of these neurons is rapidly suppressed in pregnancy and this was maintained throughout early lactation. Deletion of Prlr from arcuate kisspeptin neurons resulted in early reactivation of episodic activity of kisspeptin neurons prior to a premature return of reproductive cycles in early lactation. These observations show dynamic variation in arcuate kisspeptin neuronal activity associated with the hormonal changes of pregnancy and lactation, and provide direct evidence that prolactin action on arcuate kisspeptin neurons is necessary for suppressing fertility during lactation.

42 **Introduction**

43 In mammals, lactation is accompanied by a period of infertility. This adaptive change
44 establishes appropriate birth spacing to enable maternal metabolic resources to be directed
45 towards caring for the new-born offspring, rather than supporting another pregnancy [1].
46 Lactational infertility is characterized by a lactation-induced suppression of pulsatile
47 luteinizing hormone (LH) secretion, and the temporary loss of the reproductive cycle (in
48 rodents this is exhibited as an extended period of diestrus or anestrus) [2-5]. Lactation is also
49 characterised by chronically elevated levels of the anterior pituitary hormone prolactin, which
50 is essential for milk production and promotes adaptive changes in maternal physiology and
51 behaviour [1, 2, 4, 5]. Despite hyperprolactinaemia being a well-recognized cause of infertility,
52 the specific role that prolactin plays in lactational infertility, as distinct from other suckling-
53 or metabolic-related cues, is currently unclear [4, 6].

54 Recent *in vivo* studies have confirmed that kisspeptin neurons in the arcuate nucleus of the
55 hypothalamus are responsible for the periodic release of gonadotrophin-releasing hormone
56 (GnRH) and subsequent pulsatile luteinising hormone (LH) secretion that drives reproductive
57 function [7-11]. Studies using GCaMP6 fibre photometry in conscious mice have demonstrated
58 that the arcuate kisspeptin neuronal population exhibits episodes of increased intracellular
59 calcium levels coincident with, and immediately preceding, each pulse of LH secretion in
60 intact and gonadectomised male and female mice [7, 8 9]. Miniscope investigation showed that
61 individual kisspeptin neurons within the arcuate population act in a coordinated,
62 synchronised, and episodic manner [10, 11]. Loss of pulsatile LH secretion during lactation and
63 consequent lactational infertility may be caused by the loss of kisspeptin-mediated
64 stimulation of GnRH secretion [12-18]. Kisspeptin expression is markedly suppressed in
65 lactation [12, 16] and when exogenously stimulated, kisspeptin neurons are unable to activate
66 GnRH neurons during lactation, likely due to a lack of kisspeptin synthesis [13].

67 It is well established that hyperprolactinemia causes infertility, and thus, the elevated
68 prolactin present in lactation seems a likely candidate to be involved in suppressing fertility
69 during lactation. Prolactin administration acutely suppresses LH secretion [19], and chronic
70 exposure to elevated prolactin reduces *Kiss1* mRNA expression in the arcuate nucleus [17, 20, 21].
71 In lactating mice, suppressing endogenous prolactin secretion shortens the period of
72 infertility [22], suggesting that prolactin is important for maintaining the suppression of
73 pulsatile LH secretion during lactation. Such a role for prolactin is controversial [4, 6, 23-27],

however, with studies in a number of species suggesting that the neural stimulation of suckling may be more important in maintaining lactational infertility [28, 29]. However, it has previously been difficult to disentangle the specific role of prolactin, as suckling, prolactin, and milk production are so tightly linked that manipulating one ultimately impacts the others, making it difficult to determine the contribution of any one element. Here, using a conditional deletion strategy, we have blocked prolactin action in the brain leaving suckling, lactation, and maternal behaviour intact. Using GCaMP fibre photometry techniques, we have also documented arcuate kisspeptin neuron activity across pregnancy and lactation transitions in the same mice and established that prolactin directly acts on these neurons to suppress fertility in lactation.

85 **Materials and Methods**

86 **Animals**

87 All experiments were performed using adult female mice on a C57BL/6J background (8-20
88 weeks of age). Mice were housed under controlled temperature (22 °C ± 2°C) and lighting
89 (12-hour light/12-hour dark schedule, with lights on at 0600 hours) with *ad libitum* access to
90 food and water (Teklad Global 18% Protein Rodent Diet 2918; Envigo, Huntingdon, United
91 Kingdom). Daily body weight was recorded and vaginal cytology was used to monitor the
92 estrous cycle stage. All experiments were carried out with approval from the University of
93 Otago Animal Welfare and Ethics Committee.

94 Mice were mated with male wild-type C57BL/6J mice (presence of sperm plug = day 1
95 pregnancy). The first day a litter was seen was counted as day 1 of lactation and maternal
96 mice were left undisturbed till day 3 of lactation, when vaginal monitoring would resume and
97 litter size was normalised to 6 pups per animal, unless otherwise stated.

98 To monitor pulsatile secretion of LH, serial tail tip blood sampling and measurement of LH
99 by ELISA was undertaken as reported previously [19, 30, 31]. As novel exposure and restraint
100 stress has been shown to suppress pulsatile LH secretion [32], all mice were habituated to the
101 tail tip blood sampling procedure in a gentle restraint device (soft cardboard tube) or hand,
102 for at least 3 weeks prior to experimentation [33]. Sequential whole blood samples (4µl) were
103 collected in 6 minute intervals for 3 hours between 0900 and 1200 hours unless otherwise
104 stated. Samples were immediately diluted in 48ul 0.01M PBS/0.05% Tween 20, and frozen
105 on dry ice before being stored at -20°C for subsequent LH measurement.

106 **Effect of neuron-specific deletion of the prolactin receptor gene on the maintenance of**
107 **lactational infertility**

108 To investigate whether prolactin action in the brain is required for lactational infertility,
109 neuron-specific *Prlr* knockout mice ($Prlr^{lox/lox}/Camk2a^{Cre}$) and their respective Cre-negative
110 controls ($Prlr^{lox/lox}$) were generated, as previously described [34]. We have previously shown
111 that while $Prlr^{lox/lox}/Camk2a^{Cre}$ mice do not have a complete Prlr deletion in the forebrain,
112 there are areas of extensive deletion (as measured by reduced prolactin-induced pSTAT5),
113 such as the arcuate nucleus and ventromedial nucleus of the hypothalamus, and areas where
114 Prlr is reduced by about 50% such as the medial pre-optic area [34, 35]. RNAscope in-situ

115 hybridization was done to confirm knockdown. Briefly, intact diestrous mice and 14 day
116 OVX mice (all aged 8-16 weeks) were perfused with 2% PFA to enable visualisation of
117 kisspeptin cell bodies in both the RP3V and ARC regions (as kisspeptin cell bodies are only
118 visible in the RP3V of intact mice and in the ARC of OVX mice, due to estradiol regulation
119 [36]). Brain sections (14µm-thick) were prepared, thaw mounted onto superfrost-plus
120 microscope slides and then stored at -80°C. RNAscope in-situ hybridization was performed
121 using the RNAscope 2.5 High definition Duplex Detection kit – chromogenic (Advanced Cell
122 Diagnostics, Hayward, CA) largely in accordance with manufacturer's instruction. The
123 channel 1 Prlr probe was custom designed to pick up only the long form of the prolactin
124 receptor. It was designed to transcript NM_011169.5 with a target sequence spanning
125 nucleotides 1107-2147 (Ref: 588621; Advanced Cell Diagnostics, Hayward, CA). The
126 channel 2 Kiss1 probe was custom designed to transcript NM_178260.3 with a target
127 sequence spanning nucleotides 5 to 485 (Ref: 500141-C2; Advanced Cell Diagnostics,
128 Hayward, CA). Sections were thawed at 55°C, postfixed for 3 minutes in 2% PFA, washed in
129 0.01M PBS for 5 minutes, and endogenous peroxidases were blocked with a hydrogen
130 peroxidase solution for 10 minutes. Tissue was washed in distilled water (dH2O) (3x 2
131 minutes), then immersed in 100% ethanol briefly, air dried for 5 minutes, and a hydrophobic
132 barrier was applied. Tissue was permeabilized with RNAscope protease plus for 30 minutes
133 at 40°C. Sections were washed (2x 2 minutes) and were hybridized with the Prlr and Kiss1
134 probes (1:300 dilution, Prlr:Kiss1) or negative control probe (Cat#320751; Advanced Cell
135 Diagnostics, Hayward, CA) at 40°C for 2 hours. Amplification (Amp 1-6) was performed in
136 accordance with the manufacturer's instructions. Sections were then hybridized with a Fast-
137 RED (1:60, Fast-RED B:Fast-RED A) for 10 minutes at room temperature, before
138 undergoing further amplification steps (Amp 7-10) in accordance to manufacturer's
139 instructions. The final positive hybridization was detected by incubation with the secondary
140 detection reagents (1:50, Fast-GREEN B:Fast-GREEN) for 10 minutes at room temperature.
141 Sections were washed, counterstained with haematoxylin (25% Gills), dried at 60°C for 20
142 minutes, and cover-slipped with VectaMount (Vector laboratories, H-5000) before imaging
143 as previously described. Quantification of the proportion of kisspeptin neurons co-expressing
144 *Prlr* mRNA was undertaken in FIJI software (National Institute of Health, Bethesda,
145 Maryland, USA) following image acquisition. The total number of *Kiss1*-expressing cells and
146 the total number of these that showed *Prlr* mRNA expression were counted.
147 $Prlr^{lox/lox}/Camk2a^{Cre}$ mice showed a significant decrease in the percentage of *Kiss1*-
148 expressing cells co-expressing *Prlr* compared to controls in both the RP3V ($p = <0.0001$) and

149 arcuate nucleus (p = 0.0009) (unpaired two-tailed t tests, Supplementary Figure 1A-D). The
150 *Prlr*$^{lox/lox}$/*Camk2a*^{Cre} mice are hyperprolactinaemic due to impaired negative feedback of
151 prolactin on hypothalamic dopamine neurons [34] and therefore show disrupted estrous cycles
152 (showing recurrent pseudopregnancy-like cycles with long periods of diestrus of
153 approximately 14 days between estrus stages). However, these mice are able to become
154 pregnant and have normal pregnancies. All mice were given a 250µl subcutaneous injection
155 of bromocriptine (5mg/kg, 5% ethanol/saline; Tocris Bioscience Cat#0427) prior to being
156 mated. This treatment was designed to reinstate an estrous cycle in *Prlr*$^{lox/lox}$/*Camk2a*^{Cre} mice.
157 Bromocriptine is an agonist for the type 2 dopamine receptor and inhibits prolactin secretion
158 from the pituitary gland [37], thereby terminating the pseudopregnancy-like state and bringing
159 the mice into proestrus the following day. Following treatment, all mice were then housed
160 with a stud male.

161 For *Prlr*$^{lox/lox}$/*Camk2a*^{Cre} mice, estrous cycles were monitored from day 3 of lactation until the
162 first day of diestrus following a day of estrus (proestrus and estrus had to be observed prior to
163 transcardial perfusion on the first day of diestrus). Brains were collected following
164 transcardial perfusion for assessment of kisspeptin immunoreactivity. For every lactating
165 *Prlr*$^{lox/lox}$/*Camk2a*^{Cre} mouse (n = 8), the brain of a *Prlr*$^{lox/lox}$ control mouse (n = 8) of the
166 equivalent day (±1) of lactation was also collected. A group of non-lactating (NL) mice of
167 both genotypes (n = 5-6) was also perfused for immunohistochemistry on diestrus.

168 To evaluate pulsatile LH secretion in early lactation (prior to the return of estrous cycles) and
169 to determine whether progesterone played any role in regulating pulsatile LH secretion in
170 lactation, additional groups of lactating *Prlr*$^{lox/lox}$/*Camk2a*^{Cre} and *Prlr*$^{lox/lox}$ control mice were
171 generated and treated with either the progesterone receptor antagonist, mifepristone (4mg/kg
172 in sesame oil, s.c.; AK Scientific Inc Cat#J10622), or vehicle (n = 7-8 per group) on the
173 morning of day 4 of lactation and on day 5 of lactation, 30 minutes prior to blood sampling
174 that day. This dose was selected as it was found to be sufficient to cause termination of
175 pregnancy in wild-type C57BL/6J mice (p = 0.0072, Chi-squared test, Supplementary Figure
176 2A; pilot study) and neither vehicle nor mifepristone treatment had an effect on litter weight
177 gain (interaction of time x genotype & treatment p = 0.5322, two-way repeated measures
178 ANOVA, Supplementary Figure 2B).

179 **Measurement of LH concentrations**

180 An established sandwich ELISA method was used to determine LH concentration in diluted
181 whole blood samples collected from mice [30, 31]. Briefly, a 96-well high plate was incubated
182 with bovine monoclonal antibody (LHβ518b7, 1:1000 in 1xPBS; Dr. L. Sibley, UC Davis,
183 CA, USA) for 16 h at 4°C. Following incubation of standards, controls and experimental
184 samples for 2 hours, plates were incubated in rabbit polyclonal LH antibody (AFP240580Rb;
185 1:10,000; National Hormone and Pituitary Program, NIH) for 90 minutes, followed by
186 incubation with polyclonal goat anti-rabbit IgG/HRP antibody (1:1000; DAKO Cytomation)
187 for 90 minutes. Finally, plates were incubated in OPD (o-phenylenediamine capsules; Sigma-
188 Aldrich Cat#P7288) for 30 minutes. A standard curve for the detection of LH concentration
189 was generated using serial dilutions of mouse LH-reference preparation peptide (National
190 Hormone and Pituitary Program, NIH). Luteinizing hormone levels were read using a
191 standard absorbance plate reader (SpectraMax ABS Plus; Molecular Devices) at 490nm and
192 630nm wavelengths.

193 PULSAR Otago was used to define LH pulses [38]. Parameters used; Smoothing 0.7, Peak split
194 2.5, Level of detection 0.04, Amplitude distance 3, Assay variability 0, 2.5, 3.3, G(1)=3.5,
195 G(2)=2.6, G(3)=1.9, G(4)=1.5, G(6)=1.2. Mean LH levels were calculated by averaging all
196 LH levels collected during the experiment. The assay had a sensitivity of 0.04ng/ml to
197 4ng/ml, with an intra-assay coefficient of variation of 4.40% and an inter-assay coefficient of
198 variation of 8.29%. See supplementary information, figure 1, for all individual LH profiles.

199 **Assessment of kisspeptin expression**
200
201 ***Perfusion and fixation of tissue***

202 Mice were anaesthetised with sodium pentobarbital (15mg/mL) and transcardially perfused
203 with 4% paraformaldehyde. Brains were removed, postfixed in the same solution, and
204 cryoprotected overnight in 30% sucrose before being frozen at -80°C. Two sets of 30µm
205 thick coronal brain sections were cut using a sliding microtome, from Bregma 1.10mm to -
206 2.80mm. Brain sections were kept in cryoprotectant solution (pH = 7.6) at -20°C until
207 immunohistochemistry was performed.

208 ***Immunohistochemistry***

209 Immunohistochemistry for kisspeptin in the RP3V and arcuate nucleus was performed as
210 previously described [39]. Briefly, sections were incubated in polyclonal rabbit anti-kisspeptin

211 primary antibody (AC 566, 1:10,000; gift from A. Caraty, Institut National de la Recherche
212 Agronomique, Paris, France) for 48 hours at 4°C. Sections were then incubated with
213 biotinylated goat anti-rabbit IgG (1:200, Vector biolabs, Peterborough, GK) for 90 min at
214 room temperature, followed by incubation in an avidin-biotin complex (Elite vectastain ABC
215 kit, Vector laboratories). The bound antibody-peroxidase complex was visualised using a
216 nickel-enhanced diaminobenzidine (DAB) reaction, to form a black cytoplasmic precipitate.

217 Brain sections were imaged using an Olympus BX51 light microscope and Olympus
218 UPlanSApo 10/20x lenses. Quantification of kisspeptin neurons in the RP3V, was undertaken
219 by manually counting all labelled neurons present in all three subdivisions, the anteroventral
220 periventricular nucleus (AVPV), rostral preoptic periventricular nucleus (rPVpo), and caudal
221 preoptic periventricular nucleus (cPVpo, bregma 0.02) (2 sections per brain region per
222 mouse) and then averaging this for each animal. As kisspeptin cell bodies in the arcuate
223 nucleus were not easily observed, as previously reported [40], kisspeptin fibre immunoreactivity
224 was imaged using a Gryphax NAOS colour camera (Jenoptik) and evaluated using FIJI
225 software and the voxel counter function (National Institutes of Health). Kisspeptin fibre
226 density was measured in the arcuate nucleus across the three subdivisions; rostral arcuate
227 (rARC), middle arcuate (mARC), and caudal arcuate (cARC) with two sections of each area
228 per animal counted, and then averaged across each animal to get total number and reported as
229 total amount of voxels per ROI (voxel fraction).

230 **Characterization of arcuate kisspeptin neuronal activity using GCaMP fibre**
231 **photometry**

232 ***Stereotaxic surgery and AAV injections***

233 Adult *Kiss1*^{Cre} or *Prlr*$^{lox/lox}$/*Kiss1*^{Cre} mice (2-3 months old) were anaesthetised with 2%
234 Isoflurane, given local Lidocaine (4mg/kg, s.c.) and Carprofen (5mg/kg, s.c.) and placed in a
235 stereotaxic apparatus. A custom-made unilateral Hamilton syringe apparatus holding one
236 Hamilton syringe was used to perform unilateral injections into the arcuate nucleus. The
237 needles were lowered into place (-0.14mm A/P, +0.04mm M/L, -0.56mm DV) over 2
238 minutes and left in situ for 3 minutes before injection was made. 1µl AAV9-CAG-FLEX-
239 GCaMP6s-WPRE-SV40 ($1.3x10^{-13}$ GC/ml, University of Pennsylvania Vector Core,
240 Philadelphia, PA, USA) was injected into the arcuate nucleus at a rate of ~100nl/min with the
241 needles left in situ for 3 minutes prior to being withdrawn over a period of 6 minutes. This

242 was followed by implantation of a unilateral indwelling optical fibre (400 µm diameter, 6.5
243 mm long, 0.48 numerical aperture (NA), Doric Lenses, Canada, product code:
244 MFC_400/430-0.48_6.5mm_SM3*_FLT) at the same coordinates. Carprofen (5mg/kg body
245 weight, s.c.) was administered for post-operative pain relief. After surgery, mice received
246 daily handling and habituation to the photometry recording procedure over 4-6 weeks before
247 experimentation began.

248 ***GCaMP6 fibre photometry***

249 Photometry was performed as reported previously [9]. Fluorescence signals were acquired
250 using a custom-built fibre photometry system made primarily from Doric components. Violet
251 (405nm) and blue (490nm) fibre-coupled LEDs were sinusoidally modulated at 531 and 211
252 Hz, respectively, and focused into a 400µm, 0.48 numerical aperture fibre optic patch cord
253 connected to the mouse. Emitted fluorescence was collected by the same fibre and focused
254 onto a femtowatt photoreceiver (2151, Newport). The two GCaMP6s emission signals were
255 collected at 10 Hz in a scheduled 5s on/15s off mode by demodulating the 405nm (non-
256 calcium dependent) and 490nm (calcium dependent) signals. The power output at the tip of
257 the fibre was set at 50µW. Fluorescent signals were acquired using a custom software
258 acquisition system (Tussock Innovation, Dunedin, New Zealand) and analysed using custom
259 templates created by Dr Joon Kim (University of Otago, Dunedin, New Zealand) based on
260 mathematics and calculations similar to those previously described [41, 42]. Briefly, the
261 fluorescent signal obtained after stimulation with 405nm light was used to correct for
262 movement artefacts as follows: first, the 405nm signal was filtered using a savitzky-golay
263 filter and fitted to the 490nm signal using least linear square regression. The fitted 405nm
264 signal was then subtracted and divided from the 490nm signal to obtain the movement and
265 bleaching corrected signal. The output of these templates is 490- adjusted405/adjusted405,
266 which was multiplied to get the final ΔF/F as a percentage increase (all photometry data
267 reported as ΔF/F(%)).

268 All recordings were obtained from freely behaving mice for up to 24 hours and occurred
269 between the hours of 0800 hours and 1200 hours (apart from 24 hours post weaning
270 recording (0900 hours to 1700 hours), and day 18/19 pregnancy recording (1800 hours to
271 0800 hours the following day). Synchronized events (SE) were defined as when ΔF/F
272 exceeds 3 standard deviations (SD) above the trace mean. Manual event shape analysis was
273 performed in addition to standard deviation method for certain datasets where necessary.

274 Events were counted manually to determine frequency of events per 60 minutes. The between
275 animal variability in total signal means that changes in SE amplitude can only be reported as
276 relative changes within an animal. Relative SE amplitude was calculated by using normalised
277 ΔF/F data and then subtracting the peak of an SE from the nearest nadir to the rise of the SE
278 and averaging that for the number of SEs in a recording. To obtain normalised ΔF/F, three
279 pre-pregnancy datasets from each mouse were used to find the average maximum ΔF/F for
280 that mouse. All datasets were then divided by that normalisation value to get normalised
281 ΔF/F for each trace for each individual mouse.

282 ***Monitoring the activity of arcuate kisspeptin neurons across different reproductive stages***
283 ***in the same mice***

284 Adult *Kiss1*^{Cre} mice were 8-10 weeks of age at the beginning of experiments, and up to 12
285 months in age by time of final recording (n = 8 during pregnancy, n = 6 during lactation; 2
286 mice were euthanised due to dystocia therefore those mice were only followed through
287 pregnancy). Monitoring of vaginal cytology and weights was continuous from 1 week pre-
288 surgery till day 19 of pregnancy and resumed on day 3 of lactation (with all handling stopped
289 on day 19 to avoid potential compromise of parturition and onset of maternal behaviour). To
290 investigate the activity of the arcuate kisspeptin population across different reproductive
291 states in the same animal, the following recording protocol was followed for all *Kiss1*^{Cre}
292 mice, unless otherwise stated; virgin (diestrus), day 4 of pregnancy, day 14 of pregnancy, day
293 18/19 of pregnancy (overnight), day 7 of lactation, day 14 of lactation, day 18 of lactation, 24
294 hours after weaning, first diestrus after estrous cycles begin following weaning, and 10 days
295 after OVX. In addition, blood sample collection for paired LH measurement was done in
296 virgin (diestrus) state, on day 14 of pregnancy (in 4 mice, maximum of 6 samples were
297 collected around small "peaks" in baseline), day 7 of lactation, and day 14 of lactation. Blood
298 sampling was not carried out at additional time points as blood sampling was undertaken at
299 least a week apart, and stress from repeated sampling was attempted to be kept at a minimum
300 e.g., not blood sampling around the time of birth. Fibre photometry recordings were usually
301 between 2-4 hours in length. The only longer recordings were undertaken on day 18/19 of
302 pregnancy (14 hours) and 24 hours after weaning (8 hours). These particular recording
303 sessions were extended to determine whether there were any longer-term changes occurring
304 in the activity of the arcuate kisspeptin population in the lead up to parturition or following

305 weaning of pups (states closely followed by postpartum estrus and resumption of normal
306 estrous cycles, respectively).

307 **Effect of arcuate kisspeptin neuron-specific deletion of the prolactin receptor gene on**
308 **the maintenance of lactational infertility and the activity of kisspeptin neurons during**
309 **lactation**

310 Kisspeptin-specific prolactin-receptor knockout mice (*Prlr*$^{lox/lox}$/*Kiss1*^{Cre} [19]) and their
311 respective Cre-negative controls (*Prlr*$^{lox/lox}$) were generated. RNAscope in-situ hybridization
312 was done to confirm knockdown, with *Prlr*$^{lox/lox}$/*Kiss1*^{Cre} mice showing a significant decrease
313 in the percentage of *Kiss1*-expressing cells co-expressing *Prlr* compared to controls in the
314 arcuate ($p = <0.0001$, unpaired two-tailed t test, Extended data Figure 3E, F). Similar to
315 experiments described above, *Prlr*$^{lox/lox}$/*Kiss1*^{Cre} (n = 27) and *Prlr*$^{lox/lox}$ control (n = 30) dams
316 underwent estrous cycle monitoring from day 3 of lactation onwards to determine whether
317 mice showed an early resumption of estrus cycles.

318 To determine whether the deletion of the prolactin receptor from arcuate kisspeptin neurons
319 led to early reactivation of these neurons during lactation, adult *Prlr*$^{lox/lox}$/*Kiss1*^{Cre} mice (n =
320 5) and an additional *Kiss1*^{Cre} control mouse (n = 1) (8 weeks old at the start of the
321 experiment, and up to 14 months at end of final recording timepoint) were set up for fibre
322 photometry, as described above. Monitoring of vaginal cytology and weights was continuous
323 from 1 week pre-surgery till day 18 of pregnancy and resumed on day 3 of lactation.
324 Recordings were undertaken in a similar timeline as described above, however no pregnancy
325 recordings were done, and in early lactation recordings were performed every 2 days from
326 day 3 to day 9 of lactation, before following the same protocol as described. No blood
327 samples were taken over this lactation period in this genotype. As described previously,
328 recordings were kept between 2-4 hours, apart from the 24 hours after weaning recording (8
329 hours).

330 **Statistical analysis**

331 Data are presented as mean ± SEM and all statistical analysis was performed with PRISM
332 software 10 (GraphPad Software, San Diego, CA, USA) with a p value of < 0.05 considered
333 as statistically significant. Individual symbols in graphs represent individual mice.
334 Differences in kisspeptin cells number or fibre density was assessed using two-way

ANOVAs with Tukey's multiple comparisons tests or t tests, with both analyses using combined averages of each animal (averaged number of cells or fibre density across the three subdivisions of each nucleus to get total number reported). Resumption of estrous cycles was analysed using Log-rank (Mantel-Cox) test chi square test. LH pulse frequency data and mean LH data was analysed using two-way ANOVAs with Tukey's multiple comparisons tests. SE frequency and amplitude throughout reproductive cycles was analysed using mixed effect analysis (fixed type III) with Tukey's multiple comparisons tests where appropriate and day 18/19 of pregnancy data was analysed using t tests. Correlation between SE occurrence and LH pulses was assessed using chi-square test. All fibre photometry data used for quantitative analysis and comparison were from the first pregnancy and lactation. A full list of probability values, inferential statistics, and degrees of freedom for all data can be found in Supplementary Table 1.

348 **Results**

349 **Prolactin action on forebrain neurons is necessary to maintain lactational infertility**

350 Lactation has previously been associated with a marked decrease in *Kiss1* mRNA levels in
351 both rostral periventricular region of the third ventricle (RP3V) and arcuate nucleus
352 populations during lactation [13]. To determine whether prolactin is involved in the
353 maintenance of lactational anestrus, the *Prlr* gene was knocked out of *Camk2a* expressing
354 neurons (most forebrain neurons, as described in [34]) of female mice. Control $Prlr^{lox/lox}$ mice
355 showed a marked reduction in kisspeptin cell body immunoreactivity in the RP3V of
356 lactating compared to virgin mice (p = 0.0100, *Post hoc* Tukey's multiple comparisons test,
357 Figure 1A, C). In contrast, lactation-induced suppression of kisspeptin cell bodies in the
358 RP3V and fibre labelling in the arcuate nucleus was absent in $Prlr^{lox/lox}/Camk2a^{Cre}$ mice (p =
359 0.6409, *Post hoc* Tukey's multiple comparisons test, Figure 1A, C; interaction between
360 reproductive state and genotype p = 0.0034, two-way ANOVA, Figure 1A, C; p = 0.0020,
361 unpaired two tailed t test, measured as percentage voxels within the region of interest, Figure
362 1B, D).

363 Estrous cycles during lactation were significantly altered by deletion of Prlr in the forebrain,
364 with all $Prlr^{lox/lox}/Camk2a^{Cre}$ mice showing a return to estrus between day 6 and day 10 of
365 lactation (Figure 1E), while, as normal, estrus did not occur until day 20 in control $Prlr^{lox/lox}$
366 mice (p = <0.0001, log-rank (Mantel-Cox) test, Figure 1E). No differences in litter weight
367 gain from day 3 to day 8 of lactation were observed in either group (p = 0.3282, mixed
368 analysis test, Supplementary Figure 3), indicating that the suckling stimulus that mice
369 received was maintained in the absence of *Prlr* expression in *Camk2a* expressing neurons.
370 Collectively, these data show that prolactin action in the brain is absolutely required for the
371 lactation-induced suppression of kisspeptin expression and to maintain lactational infertility
372 in mice.

373 In a separate cohort of mice, pulsatile LH secretion in $Prlr^{lox/lox}/Camk2a^{Cre}$ mice was
374 monitored in early lactation, prior to the return of estrous cycles. To rule out a potential role
375 for progesterone in suppressing fertility during lactation [9, 43, 44], the progesterone receptor
376 antagonist mifepristone (RU486), was administered to mice in early lactation. Vehicle-treated
377 $Prlr^{lox/lox}$ control mice showed the expected near complete absence of pulsatile LH secretion
378 during lactation (Figure 2A, B). In contrast, nearly all $Prlr^{lox/lox}/Camk2a^{Cre}$ mice showed a

379 lack of the normal lactation-induced suppression of pulsatile LH secretion demonstrated by a
380 significant increase in frequency of LH pulses compared to controls (effect of genotype p =
381 0.0024, two-way ANOVA with Tukey's multiple comparisons test, Figure 2A, B). There was
382 no effect of mifepristone on this pattern of LH secretion, suggesting that progesterone action
383 is not required for the suppression of LH secretion (LH pulse frequency (interaction genotype
384 x treatment p = 0.2807; treatment p = 0.8588; Figure 2B), mean LH levels (interaction
385 genotype x treatment p = 0.8697; treatment p = 0.8586; Figure 2C), two-way ANOVA with
386 Tukey's multiple comparisons test). These data indicate that prolactin is the primary signal
387 responsible for the suppression of LH during lactation in mice. Individual LH profiles from
388 all animals are shown in Supplementary Figure 4.

389 **Episodic activity of arcuate kisspeptin neurons is suppressed during pregnancy and**
390 **most of lactation**

391 To directly assess the role of prolactin in regulating kisspeptin neuron activity during
392 lactation, GCaMP6 fibre photometry was undertaken to monitor real-time activity of arcuate
393 kisspeptin neurons in freely behaving mice. We first undertook a longitudinal assessment of
394 changes in kisspeptin neuronal activity by tracking individual animals throughout pregnancy
395 and lactation and following weaning (Figure 3).

396 Initially, GCaMP fibre photometry recordings were collected in the virgin diestrous state,
397 both with and without serial blood sampling to measure LH concentrations. As can be seen in
398 Figure 4A, photometry recordings were characterized by discrete synchronised events (SEs)
399 of elevated intracellular calcium (indicative of synchronous activity of the kisspeptin
400 population), with each SE correlating perfectly to a single pulse of LH in the minutes
401 following (p = <0.0001, chi-squared test). These were observed to be at a similar rate to that
402 described previously in diestrous mice using GCaMP photometry in a different *Kiss1* mouse
403 line [9], with periodic SEs occurring about once per hour (1.250±0.250; Figure 3 & 4B).

404 The activity of the arcuate kisspeptin population in *Kiss1*^{Cre} mice dynamically changed
405 depending on the reproductive state of the mouse (p = 0.0012, mixed-effect analysis, Figure 3
406 & 4B). On day 4 of pregnancy, SE frequency had markedly decreased (0.297±0.136/hr;
407 Figure 3 & 4B), indicating an early reduction in activity of arcuate kisspeptin neurons during
408 pregnancy. By day 14 of pregnancy, no SEs were seen (0±0/hr; Figure 3 & 4B) and this was
409 confirmed by a lack of pulsatile LH secretion (Supplementary Figure 5). In late pregnancy

410 (day 18), neuronal activity was monitored for 14 hours, during which time low amplitude,
411 SEs were unexpectedly observed at similar frequencies to virgin levels (2.043±0.940/hr;
412 Figure 3 & 4B-C). This unusual pattern of activity is illustrated in more detail in Figure 5
413 where alongside the resurgence of low amplitude SEs, there was a marked increase in
414 baseline activity observed, relative to other stages. This activity was reminiscent of the
415 miniature SEs observed to be caused by activation of subgroups of cells in a brain slice
416 technique [11], but we are unable to resolve such events using the present methods. Since our
417 aim was to continue longitudinal assessment of the arcuate kisspeptin population into
418 lactation and weaning, mice were not disrupted by blood sampling immediately prior to
419 parturition as we were concerned that this additional stressor might interfere with
420 establishment of maternal behaviour. Hence, we are unable to report whether these low
421 amplitude SEs and elevated baseline activity were associated with LH secretion.

422 Evaluation of activity of arcuate kisspeptin neurons during lactation showed complete
423 suppression of activity on day 7 of lactation with a corresponding absence of pulsatile LH
424 secretion (0±0/hr; Figure 3 & 4B). This lactation-induced suppression of activity was
425 partially relieved by day 14 of lactation (0.583±0.083/hr; Figure 3 & 4B), with SEs again
426 corresponding to low frequency pulses of LH secretion. Further increases in SE frequency
427 were seen on day 18 of lactation (0.850±0.100/hr; Figure 3 & 4B), including an increase in
428 baseline activity, similar to that seen in late pregnancy, and by 24 hours after weaning (day
429 22 postpartum) the frequency of SEs returned to close to non-pregnant levels
430 (1.375±0.114/hr; Figure 3 & 4B). Frequency remained unchanged on the day of first diestrus
431 following a return to estrous cycles after weaning (1.533±0.226/hr; Figure 3 & 4B). As a
432 final manipulation, mice were ovariectomized (OVX), and arcuate kisspeptin population
433 activity observed to increase significantly with clusters of high amplitude activity
434 (4.778±0.222/hr; Figure 3 & 4B), consistent with previous reports following OVX in
435 nulliparous mice [45]. Collectively, these observations show extensive, dynamic variation in
436 activity of the arcuate kisspeptin neuronal population associated with pregnancy and
437 lactation.

438 **Mice with an arcuate kisspeptin neuron-specific deletion have premature reactivation of**
439 **estrous cycles and neuronal activity in lactation**

440 To determine whether the prolactin-induced suppression of estrous cycles and LH pulsatile
441 secretion was specifically mediated by kisspeptin neurons, mice were generated with an

442 arcuate-specific deletion of the Prlr from kisspeptin neurons [19]. Similar to the data from
443 forebrain neuron-specific deletion of Prlr, there was early resumption of estrous cycles in
444 *Prlr*$^{lox/lox}$/*Kiss1*^{Cre} mice during lactation (63% showing estrus by day 10 of lactation and 83%
445 by day 19 lactation) compared to *Prlr*$^{lox/lox}$ controls (4% by day 19 lactation) ($p = <0.0001$,
446 log-rank (Mantel-Cox) test, Figure 6A). No difference in litter weight gain during lactation
447 (day 3-20 of lactation weight gain) was observed in either group ($p = 0.6404$, two-way
448 ANOVA, Supplementary Figure 1H) indicating that suckling and/or lactation itself was not
449 impaired. *In vivo* GCaMP6 fibre photometry in *Prlr*$^{lox/lox}$/*Kiss1*^{Cre} mice showed early
450 reactivation of the arcuate kisspeptin population between day 3 and 5 of lactation (Figure
451 6C). This was accompanied by a clear return to estrous within this early lactation window in
452 4/5 mice. These data demonstrate that prolactin action specifically on arcuate kisspeptin
453 neurons is responsible for maintaining suppression of those neurons, and thereby fertility,
454 during lactation in mice.

455 **Discussion**

456 We demonstrate here that prolactin action in arcuate kisspeptin neurons is necessary for the
457 maintained suppression of fertility during lactation in mice. Neuron-specific Prlr deletion
458 (*Prlr*$^{lox/lox}$/*Camk2a*^{Cre}) resulted in premature return to estrus in early lactation, even in the
459 presence of ongoing suckling stimulus and the full metabolic consequences of milk
460 production. Accompanying the resumption of estrus was an absence of the normal lactation-
461 induced reduction in kisspeptin immunoreactivity [12, 16, 20], and pulsatile LH secretion was also
462 observed on day 5 of lactation prior to the premature estrus when it would normally have
463 been completely absent [46-48]. To evaluate the specific role of kisspeptin neurons in mediating
464 the prolactin-induced suppression of fertility, we have comprehensively mapped the activity
465 of arcuate kisspeptin neurons throughout a full reproductive cycle: pregnancy, lactation, and
466 after weaning in individual animals. The data show an immediate suppression of activity of
467 arcuate kisspeptin neuronal activity during pregnancy, and this is maintained throughout most
468 of lactation, apart from a brief window of reactivation immediately prior to parturition.
469 Deleting Prlr specifically from arcuate kisspeptin neurons prevented the suppression of
470 activity in early lactation, resulting in premature induction of episodic activation of kisspeptin
471 neurons, and early onset of estrus. Combined, these data provide direct evidence that
472 prolactin action on kisspeptin neurons is necessary for lactation-induced infertility in mice.

473 It is now well established that the arcuate kisspeptin neurons form the GnRH "pulse
474 generator", and hence drive pulsatile release of GnRH from the hypothalamus and
475 consequent pulses of LH form the pituitary that is required for fertility [49-51]. This is the first
476 study to monitor activity of the GnRH "pulse generator" across different reproductive states
477 in the same animal, and the data largely match previously described patterns of LH secretion
478 [47, 52]. The frequency and dynamics of the synchronised events changed dramatically, initially
479 due to the pregnancy-induced changes in ovarian hormones. The abrupt decrease in "pulse
480 generator" activity in early gestation is likely caused by rising levels of progesterone, known
481 to profoundly suppress activity of arcuate kisspeptin neurons and LH secretion [9, 43, 44].
482 Progesterone is elevated throughout pregnancy, gradually increasing until luteolysis and
483 progesterone withdrawal occurs in the lead up to parturition [53-56]. Interestingly, we observed a
484 transient reactivation of the arcuate kisspeptin neurons in the night between days 18 and 19 of
485 pregnancy. This was characterised by frequent, low amplitude episodes of activity, and
486 increased baseline activity that may represent the intermittent synchronized activity of small

487 subsets of arcuate kisspeptin neurons that have not yet transitioned to full synchronization of
488 the whole population [11]. It seems likely that this pattern of activity is associated with
489 progesterone withdrawal in late pregnancy and may be important in stimulating follicular
490 growth leading up to a postpartum ovulation [57, 58].

491 In early lactation, episodic activity of arcuate kisspeptin neurons was absent, with sporadic
492 low-amplitude activity returning around day 14 of lactation. There was another period of
493 increased baseline activity in late lactation, similar to that seen in late pregnancy, potentially
494 representing a signature of reactivation of synchronized activity of the arcuate kisspeptin
495 neurons. Overall patterns of activity rapidly returned to normal diestrous levels soon after
496 weaning. This increase in "pulse generator" activity during late lactation mirrors the increase
497 in LH levels that has been reported as lactation progresses [59]. In the absence of Prlr in arcuate
498 kisspeptin neurons, however, synchronized episodic activity re-appeared as early as 3 days
499 after birth, even in the presence of ongoing suckling. These data clearly show that prolactin
500 action in the arcuate kisspeptin neurons is necessary to sustain lactational infertility in mice.
501 The observed disruption of lactational infertility in *Prlr*$^{lox/lox}$/*Kiss1*^{Cre} mice is particularly
502 remarkable given that Prlr deletion is restricted to arcuate kisspeptin neurons in this model [19],
503 and prolactin action on RP3V kisspeptin neurons [21, 60] and on gonadotrophs in the pituitary
504 gland [61-63] are unaffected.

505 The indispensable role for prolactin in mediating lactation-induced infertility in the mouse is
506 surprising, given the consensus of much work in other species concluding that other factors
507 may be more important (see [4, 6, 26, 27, 64]). This may reflect a level of redundancy amongst
508 contributing factors across all species, including ovarian hormones, metabolic cues and
509 neural inputs of suckling. Notably, the conditional deletion approach described here
510 distinguishes prolactin action from the neurogenic effects of suckling without altering the
511 process of lactation itself. Moreover, this approach avoids the potential confounding effects
512 of using dopamine agonists to suppress prolactin [28, 29], given that dopamine can directly
513 inhibit GnRH neuronal activity [65].

514 While the effects of widespread neuronal deletion (*Prlr*$^{lox/lox}$/*Camk2a*^{Cre}) on fertility were
515 largely recapitulated by the arcuate kisspeptin-specific model, it was apparent that the global
516 deletion was more effective at inducing the return to estrus during lactation (in 100% of
517 animals by day 10), compared to the arcuate kisspeptin-specific model (63% by day 10, and
518 83% by day 19). This may be due to the absence of lactation-induced suppression of *Kiss1*

expression in RP3V kisspeptin neurons of *Prlr*$^{lox/lox}$/*Camk2a*^{Cre} mice. Similarly, we cannot rule out the possibility that other populations of prolactin-sensitive neurons, such as GABA or dopamine neurons [60], may contribute to suppressing estrous cycles during lactation. Nevertheless, our data collectively provide strong evidence that prolactin action on arcuate kisspeptin neurons is the primary factor mediating lactation-induced infertility in mice. Given that hyperprolactinemia induces infertility in humans and many other species [21, 22, 66-75], it is likely that a conserved mechanism will be contributing to lactational infertility in all mammalian species.

Acknowledgments

We would like to acknowledge the research assistance of Zin Khant-Aung, genotyping by Pene Knowles, and Dr Joon Kim for his assistance with analysis of fibre photometry data.

Financial support: This work was supported by Health Research Council of New Zealand (grant number: 21-560) and the Lions Club of Dunedin South - administered by Perpetual Guardian (Otago Medical Research Foundation).

533 **References**

534 1. Short, R.V. Lactation--the central control of reproduction. *Ciba Foundation symposium*,
535 73-86 (1976).
536 2. McNeilly, A.S.*, et al.* Fertility after childbirth: pregnancy associated with breast feeding.
537 *Clin Endocrinol (Oxf)* **19**, 167-173 (1983).
538 3. Fox, S.R. & Smith, M.S. The suppression of pulsatile luteinizing hormone secretion
539 during lactation in the rat. *Endocrinology* **115**, 2045-2051 (1984).
540 4. McNeilly, A.S. Lactational control of reproduction. *Reprod Fertil Dev* **13**, 583-590
541 (2001).
542 5. Tsukamura, H. & Maeda, K. Non-metabolic and metabolic factors causing lactational
543 anestrus: rat models uncovering the neuroendocrine mechanism underlying the suckling-
544 induced changes in the mother. *Progress in brain research* **133**, 187-205 (2001).
545 6. McNeilly, A.S. Lactation and fertility. *Journal of mammary gland biology and neoplasia*
546 **2**, 291-298 (1997).
547 7. Clarkson, J.*, et al.* Definition of the hypothalamic GnRH pulse generator in mice. *Proc*
548 *Natl Acad Sci U S A* **114**, E10216-E10223 (2017).
549 8. Han, S.Y., Kane, G., Cheong, I. & Herbison, A.E. Characterization of GnRH Pulse
550 Generator Activity in Male Mice Using GCaMP Fiber Photometry. *Endocrinology* **160**,
551 557-567 (2019).
552 9. McQuillan, H.J., Han, S.Y., Cheong, I. & Herbison, A.E. GnRH Pulse Generator
553 Activity Across the Estrous Cycle of Female Mice. *Endocrinology* **160**, 1480-1491
554 (2019).
555 10. Moore, A.M., Coolen, L.M. & Lehman, M.N. In vivo imaging of the GnRH pulse
556 generator reveals a temporal order of neuronal activation and synchronization during
557 each pulse. *Proceedings of the National Academy of Sciences* **119**, e2117767119 (2022).
558 11. Han, S.Y.*, et al.* Mechanism of kisspeptin neuron synchronization for pulsatile hormone
559 secretion in male mice. *Cell Rep* **42**, 111914 (2023).
560 12. Yamada, S.*, et al.* Inhibition of metastin (kisspeptin-54)-GPR54 signaling in the arcuate
561 nucleus-median eminence region during lactation in rats. *Endocrinology* **148**, 2226-2232
562 (2007).
563 13. Liu, X., Brown, R.S., Herbison, A.E. & Grattan, D.R. Lactational anovulation in mice
564 results from a selective loss of kisspeptin input to GnRH neurons. *Endocrinology* **155**,
565 193-203 (2014).
566 14. Roa, J.*, et al.* Hypothalamic expression of KiSS-1 system and gonadotropin-releasing
567 effects of kisspeptin in different reproductive states of the female Rat. *Endocrinology*
568 **147**, 2864-2878 (2006).
569 15. Ladyman, S.R. & Woodside, B. Food restriction during lactation suppresses Kiss1
570 mRNA expression and kisspeptin-stimulated LH release in rats. *Reproduction* **147**, 743-
571 751 (2014).
572 16. True, C., Kirigiti, M., Ciofi, P., Grove, K.L. & Smith, M.S. Characterisation of arcuate
573 nucleus kisspeptin/neurokinin B neuronal projections and regulation during lactation in
574 the rat. *J Neuroendocrinol* **23**, 52-64 (2011).
575 17. Brown, R.S., Herbison, A.E. & Grattan, D.R. Prolactin regulation of kisspeptin neurones
576 in the mouse brain and its role in the lactation-induced suppression of kisspeptin
577 expression. *J. Neuroendocrinol.* **26**, 898-908 (2014).
578 18. Xu, J., Kirigiti, M.A., Grove, K.L. & Smith, M.S. Regulation of food intake and
579 gonadotropin-releasing hormone/luteinizing hormone during lactation: role of insulin
580 and leptin. *Endocrinology* **150**, 4231-4240 (2009).

19. Brown, R.S.E., *et al.* Acute Suppression of LH Secretion by Prolactin in Female Mice Is Mediated by Kisspeptin Neurons in the Arcuate Nucleus. *Endocrinology* **160**, 1323-1332 (2019).
20. Araujo-Lopes, R., *et al.* Prolactin regulates kisspeptin neurons in the arcuate nucleus to suppress LH secretion in female rats. *Endocrinology* **155**, 1010-1020 (2014).
21. Sonigo, C., *et al.* Hyperprolactinemia-induced ovarian acyclicity is reversed by kisspeptin administration. *J Clin Invest* **122**, 3791-3795 (2012).
22. Hackwell, E.C., Ladyman, S.R., Brown, R.S. & Grattan, D.R. Mechanisms of lactation-induced infertility in female mice. *Endocrinology* **164**, bqad049 (2023).
23. Schallenberger, E., Richardson, D.W. & Knobil, E. Role of prolactin in the lactational amenorrhea of the rhesus monkey (Macaca mulatta). *Biol Reprod* **25**, 370-374 (1981).
24. McNeilly, A. Suckling and the control of gonadotropin secretion. in *The Physiology of Reproduction* (ed. J.N. E. Knobil) 1179–1212 (Raven Press, New York, 1994).
25. Sugimoto, A., *et al.* Central somatostatin-somatostatin receptor 2 signaling mediates lactational suppression of luteinizing hormone release via the inhibition of glutamatergic interneurons during late lactation in rats. *Journal of Reproduction and Development* (2022).
26. Tay, C.C., Glasier, A.F. & McNeilly, A.S. Twenty-four hour patterns of prolactin secretion during lactation and the relationship to suckling and the resumption of fertility in breast-feeding women. *Human reproduction (Oxford, England)* **11**, 950-955 (1996).
27. Diaz, S., *et al.* Circadian variation of basal plasma prolactin, prolactin response to suckling, and length of amenorrhea in nursing women. *The Journal of clinical endocrinology and metabolism* **68**, 946-955 (1989).
28. Maeda, K., *et al.* Prolactin does not mediate the suppressive effect of the suckling stimulus on luteinizing hormone secretion in ovariectomized lactating rats. *Endocrinologia japonica* **37**, 405-411 (1990).
29. Smith, M.S. The relative contribution of suckling and prolactin to the inhibition of gonadotropin secretion during lactation in the rat. *Biol Reprod* **19**, 77-83 (1978).
30. Steyn, F.J., *et al.* Development of a methodology for and assessment of pulsatile luteinizing hormone secretion in juvenile and adult male mice. *Endocrinology* **154**, 4939-4945 (2013).
31. Czieselsky, K., *et al.* Pulse and Surge Profiles of Luteinizing Hormone Secretion in the Mouse. *Endocrinology* **157**, 4794-4802 (2016).
32. Briski, K.P. & Sylvester, P.W. Effects of sequential acute stress exposure on stress-induced pituitary luteinizing hormone and prolactin secretion. *Life sciences* **41**, 1249-1255 (1987).
33. Steyn, F.J., *et al.* Development of a method for the determination of pulsatile growth hormone secretion in mice. *Endocrinology* **152**, 3165-3171 (2011).
34. Brown, R.S., *et al.* Conditional Deletion of the Prolactin Receptor Reveals Functional Subpopulations of Dopamine Neurons in the Arcuate Nucleus of the Hypothalamus. *J. Neurosci.* **36**, 9173-9185 (2016).
35. Gustafson, P., *et al.* Prolactin receptor-mediated activation of pSTAT5 in the pregnant mouse brain. *J Neuroendocrinol* **32**, e12901 (2020).
36. Smith, J.T., Cunningham, M.J., Rissman, E.F., Clifton, D.K. & Steiner, R.A. Regulation of Kiss1 gene expression in the brain of the female mouse. *Endocrinology* **146**, 3686-3692 (2005).
37. Moult, P.J., Rees, L.H. & Besser, G.M. Pulsatile gonadotrophin secretion in hyperprolactinaemic amenorrhoea an the response to bromocriptine therapy. *Clin Endocrinol (Oxf)* **16**, 153-162 (1982).

38. Porteous, R.*, et al.* Reformulation of PULSAR for Analysis of Pulsatile LH Secretion and a Revised Model of Estrogen-Negative Feedback in Mice. *Endocrinology* **162** (2021).
39. Clarkson, J., d'Anglemont de Tassigny, X., Colledge, W.H., Caraty, A. & Herbison, A.E. Distribution of kisspeptin neurones in the adult female mouse brain. *J Neuroendocrinol* **21**, 673-682 (2009).
40. Clarkson, J., Boon, W.C., Simpson, E.R. & Herbison, A.E. Postnatal development of an estradiol-kisspeptin positive feedback mechanism implicated in puberty onset. *Endocrinology* **150**, 3214-3220 (2009).
41. Kim, C.K.*, et al.* Simultaneous fast measurement of circuit dynamics at multiple sites across the mammalian brain. *Nature methods* **13**, 325-328 (2016).
42. Sherathiya, V.N., Schaid, M.D., Seiler, J.L., Lopez, G.C. & Lerner, T.N. GuPPy, a Python toolbox for the analysis of fiber photometry data. *Scientific Reports* **11**, 24212 (2021).
43. Goodman, R.L. & Karsch, F.J. Pulsatile secretion of luteinizing hormone: differential suppression by ovarian steroids. *Endocrinology* **107**, 1286-1290 (1980).
44. Skinner, D.C.*, et al.* The negative feedback actions of progesterone on gonadotropin-releasing hormone secretion are transduced by the classical progesterone receptor. *Proc Natl Acad Sci U S A* **95**, 10978-10983 (1998).
45. McQuillan, H.J.*, et al.* Definition of the estrogen negative feedback pathway controlling the GnRH pulse generator in female mice. *Nature Communications* **13**, 7433 (2022).
46. Bohnet, H.G. & Schneider, H.P. Prolactin as a cause of anovulation. in *Prolactin and human reproduction* (ed. P.G. Crosignani & C. Robyn) 153-159 (Academic Press, New York, 1977).
47. McNeilly. Effects of lactation on fertility. (1979).
48. McNeilly, A.S., Tay, C.C. & Glasier, A. Physiological mechanisms underlying lactational amenorrhea. *Ann. N. Y. Acad. Sci.* **709**, 145-155 (1994).
49. Herbison, A.E. The Gonadotropin-Releasing Hormone Pulse Generator. *Endocrinology* **159**, 3723-3736 (2018).
50. de Roux, N.*, et al.* Hypogonadotropic hypogonadism due to loss of function of the KiSS1-derived peptide receptor GPR54. *Proc Natl Acad Sci U S A* **100**, 10972-10976 (2003).
51. Seminara et al. The GPR54 gene as a regulator of puberty. (2003).
52. Morishige, W.K., Pepe, G.J. & Rothchild, I. Serum luteinizing hormone, prolactin and progesterone levels during pregnancy in the rat. *Endocrinology* **92**, 1527-1530 (1973).
53. Virgo, B.B. & Bellward, G.D. Serum progesterone levels in the pregnant and postpartum laboratory mouse. *Endocrinology* **95**, 1486-1490 (1974).
54. Pointis, G., Rao, B., Latreille, M., Mignot, T.-M. & Cedard, L. Progesterone levels in the circulating blood of the ovarian and uterine veins during gestation in the mouse. *Biology of Reproduction* **24**, 801-805 (1981).
55. Bridges, R.S. A quantitative analysis of the roles of dosage, sequence, and duration of estradiol and progesterone exposure in the regulation of maternal behavior in the rat. *Endocrinology* **114**, 930-940 (1984).
56. Sugimoto, Y.*, et al.* Failure of parturition in mice lacking the prostaglandin F receptor. *Science* **277**, 681-683 (1997).
57. Thapa, S., Short, R.V. & Potts, M. Breast feeding, birth spacing and their effects on child survival. *Nature* **335**, 679-682 (1988).
58. Zakar, T. & Hertelendy, F. Progesterone withdrawal: key to parturition. *American journal of obstetrics and gynecology* **196**, 289-296 (2007).

59. Rolland, R., Lequin, R.M., Schellekens, L.A. & Jong, F.H.D. The role of prolactin in the restoration of ovarian function during the early post-partum period in the human female: I. A study during physiological lactation. *Clinical Endocrinology* **4**, 15-25 (1975).
60. Kokay, I.C., Petersen, S.L. & Grattan, D.R. Identification of prolactin-sensitive GABA and kisspeptin neurons in regions of the rat hypothalamus involved in the control of fertility. *Endocrinology* **152**, 526-535 (2011).
61. Hodson, D.J., Townsend, J. & Tortonese, D.J. Characterization of the Effects of Prolactin in Gonadotroph Target Cells1. *Biology of Reproduction* **83**, 1046-1055 (2010).
62. Tortonese, D.J., Brooks, J., Ingleton, P.M. & McNeilly, A.S. Detection of prolactin receptor gene expression in the sheep pituitary gland and visualization of the specific translation of the signal in gonadotrophs. *Endocrinology* **139**, 5215-5223 (1998).
63. Henderson, H.L., Townsend, J. & Tortonese, D.J. Direct effects of prolactin and dopamine on the gonadotroph response to GnRH. *J Endocrinol* **197**, 343-350 (2008).
64. Woodside, C. & Jans, J.E. Role of the nutritional status of the litter and length and frequency of mother-litter contact bouts in prolonging lactational diestrus in rats. *Horm Behav* **29**, 154-176 (1995).
65. Liu, X. & Herbison, A.E. Dopamine regulation of gonadotropin-releasing hormone neuron excitability in male and female mice. *Endocrinology* **154**, 340-350 (2013).
66. Greer, M.E., Moraczewski, T. & Rakoff, J.S. Prevalence of hyperprolactinemia in anovulatory women. *Obstetrics and gynecology* **56**, 65-69 (1980).
67. Evans, W., Cronin, M. & Thorner, M. Hypoganadism in hyperprolactinemia: proposed mechanisms. (1982).
68. Koike, K.*, et al.* Effect of prolactin on the secretion of hypothalamic GnRH and pituitary gonadotropins. *Hormone research* **35 Suppl 1**, 5-12 (1991).
69. Patel, S.S. & Bamigboye, V. Hyperprolactinaemia. *Journal of obstetrics and gynaecology : the journal of the Institute of Obstetrics and Gynaecology* **27**, 455-459 (2007).
70. Cohen-Becker, I.R., Selmanoff, M. & Wise, P.M. Hyperprolactinemia alters the frequency and amplitude of pulsatile luteinizing hormone secretion in the ovariectomized rat. *Neuroendocrinology* **42**, 328-333 (1986).
71. Sarkar, D.K. & Yen, S.S. Hyperprolactinemia decreases the luteinizing hormone-releasing hormone concentration in pituitary portal plasma: a possible role for beta-endorphin as a mediator. *Endocrinology* **116**, 2080-2084 (1985).
72. Fox, S.R., Hoefer, M.T., Bartke, A. & Smith, M.S. Suppression of pulsatile LH secretion, pituitary GnRH receptor content and pituitary responsiveness to GnRH by hyperprolactinemia in the male rat. *Neuroendocrinology* **46**, 350-359 (1987).
73. Park, S.K., Keenan, M.W. & Selmanoff, M. Graded hyperprolactinemia first suppresses LH pulse frequency and then pulse amplitude in castrated male rats. *Neuroendocrinology* **58**, 448-453 (1993).
74. Park, S.K. & Selmanoff, M. Dose-dependent suppression of postcastration luteinizing hormone secretion exerted by exogenous prolactin administration in male rats: a model for studying hyperprolactinemic hypogonadism. *Neuroendocrinology* **53**, 404-410 (1991).
75. Grattan, D.R., Jasoni, C.L., Liu, X., Anderson, G.M. & Herbison, A.E. Prolactin regulation of gonadotropin-releasing hormone neurons to suppress luteinizing hormone secretion in mice. *Endocrinology* **148**, 4344-4351 (2007).

727 **Figures**

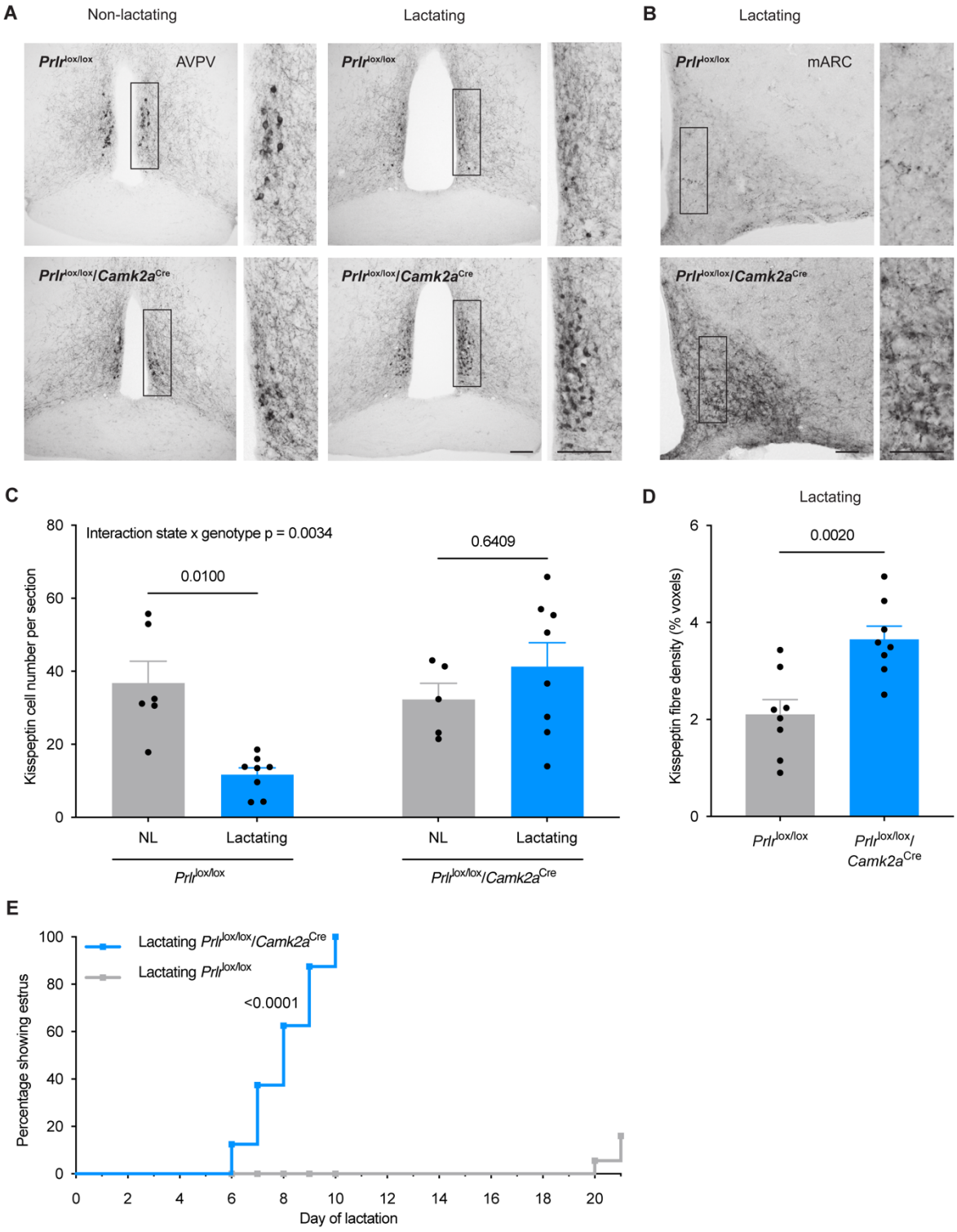

728

729

730 **Figure 1. *Prlr*$^{lox/lox}$/*Camk2a*^{Cre} mice do not undergo the normal period of lactational**
731 **infertility and the lactation-induced suppression of kisspeptin immunoreactivity is**
732 **absent.** (A) Kisspeptin immunoreactivity shown in representative photomicrographs from the
733 rostral periventricular region of the third ventricle (RP3V) non-lactating (NL; left) and
734 lactating (right) *Prlr*$^{lox/lox}$ control and *Prlr*$^{lox/lox}$/*Camk2a*^{Cre} mice (from anteroventral
735 periventricular nucleus (AVPV) region of RP3V). (B) Representative photomicrographs
736 showing mid arcuate nucleus (mARC) of a lactating *Prlr*$^{lox/lox}$ mouse (top) and a lactating
737 *Prlr*$^{lox/lox}$/*Camk2a*^{Cre} mouse (bottom). (C) Total kisspeptin cell number for the RP3V (NL
738 *Prlr*$^{lox/lox}$ (n = 6) versus lactating *Prlr*$^{lox/lox}$ control (n = 8) p = 0.0100, NL *Prlr*$^{lox/lox}$/*Camk2a*^{Cre}
739 (n = 5) versus lactating *Prlr*$^{lox/lox}$/*Camk2a*^{Cre} (n = 8) p = 0.6409). Two-way ANOVA followed
740 by Tukey's multiple comparisons test. (D) Quantification of kisspeptin fibre density in the
741 arcuate nucleus (Fiji software, measured in percentage voxels per region of interest), showing
742 total kisspeptin fibre density in the arcuate nucleus (lactating *Prlr*$^{lox/lox}$ control n = 8, lactating
743 *Prlr*$^{lox/lox}$/*Camk2a*^{Cre} n = 7, p = 0.0020, unpaired two-tailed t test). (E) *Prlr*$^{lox/lox}$/*Camk2a*^{Cre}
744 mice (blue, n = 8) resume estrous cycles significantly earlier (100% within 6-10 days of
745 lactation) than *Prlr*$^{lox/lox}$ controls (grey, n = 10) (p = <0.0001, Log-rank (Mantel-Cox) test).
746 Scale bar image and insert = 50μm. Values are shown as mean ± SEM.

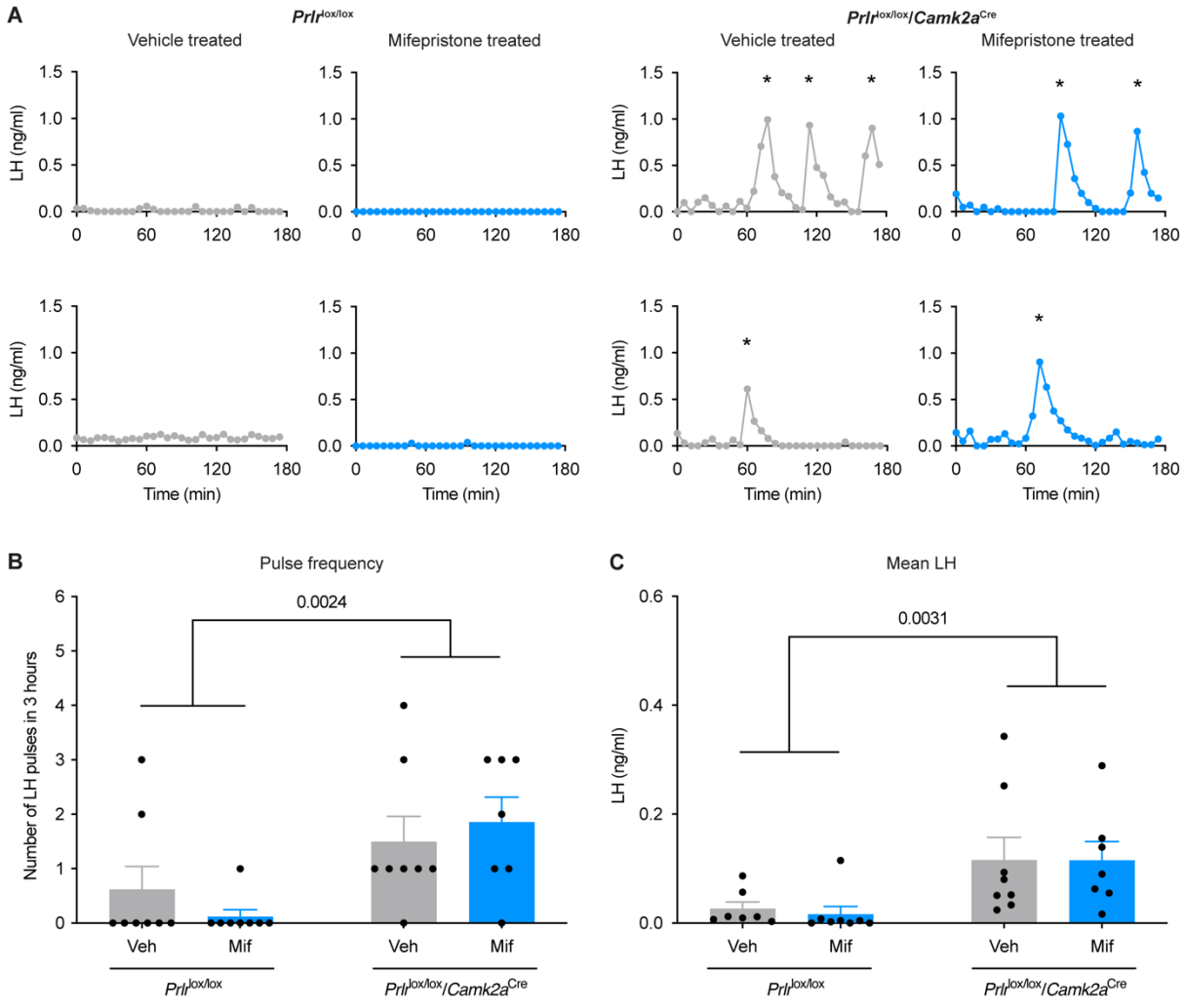

Figure 2. Prolactin action in the brain during lactation is necessary for the suppression of pulsatile LH secretion. Examples of pulsatile LH levels in the blood from lactating *Prlr*$^{lox/lox}$ controls and lactating *Prlr*$^{lox/lox}$/*Camk2a*^{Cre} mice that have either been treated with vehicle (sesame oil, s.c., grey, veh) or 4mg/kg mifepristone (in sesame oil, s.c., blue, mif) on the day prior and on the day of blood sampling (2 injections). Asterisks indicate LH pulse peaks as detected by PULSAR Otago analysis. Graphs show LH pulse frequency (B; interaction p = 0.2807, genotype p = 0.0024, state p = 0.8558), and mean LH levels (C; interaction p = 0.8697, genotype p = 0.0031, state p = 0.8586). Lactating vehicle-treated *Prlr*$^{lox/lox}$ (n = 8), lactating mifepristone-treated *Prlr*$^{lox/lox}$ (n = 8), lactating vehicle-treated *Prlr*$^{lox/lox}$/*Camk2a*^{Cre} (n = 8), lactating mifepristone-treated *Prlr*$^{lox/lox}$/*Camk2a*^{Cre} (n = 7). Two-way ANOVA followed by Tukey's multiple comparisons test. Values are shown as mean ± SEM.

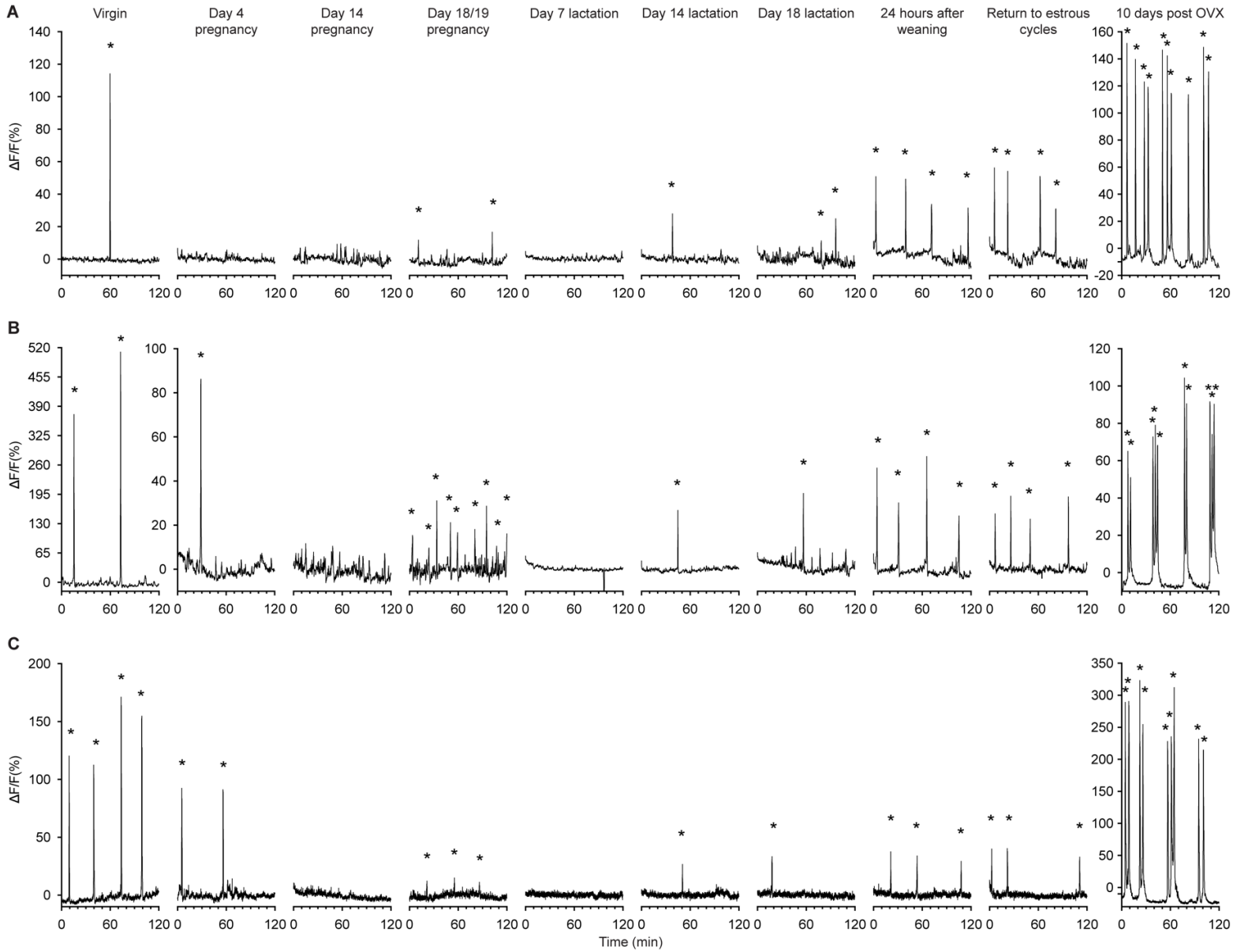
A
B
C
Virgin
Day 4 pregnancy
Day 14 pregnancy
Day 18/19 pregnancy
Day 7 lactation
Day 14 lactation
Day 18 lactation
24 hours after weaning
Return to estrous cycles
10 days post OVX
ΔF/F(%)
Time (min)

762 **Figure 3. Arcuate kisspeptin neuron GCaMP6 population activity throughout different**
763 **reproductive states in the same mice.** Representative neuronal activity from three *Kiss1*^{Cre}
764 mice throughout the virgin, pregnant, lactating, and post-weaning states. The time points
765 monitored in order were: virgin diestrus, day 4 pregnancy, day 14 pregnancy, day 18/19
766 pregnancy (overnight), day 7 lactation, day 14 lactation, day 18 lactation, 24 hours after
767 weaning (day 22 postpartum), return to normal cycling following weaning (return to estrous
768 cycles), and 10 days post ovariectomy (OVX). Asterisks indicate SEs. Note: dataset from (B)
769 on day 4 of pregnancy onwards and OVX datasets from all mice are on a different y axes
770 scale.

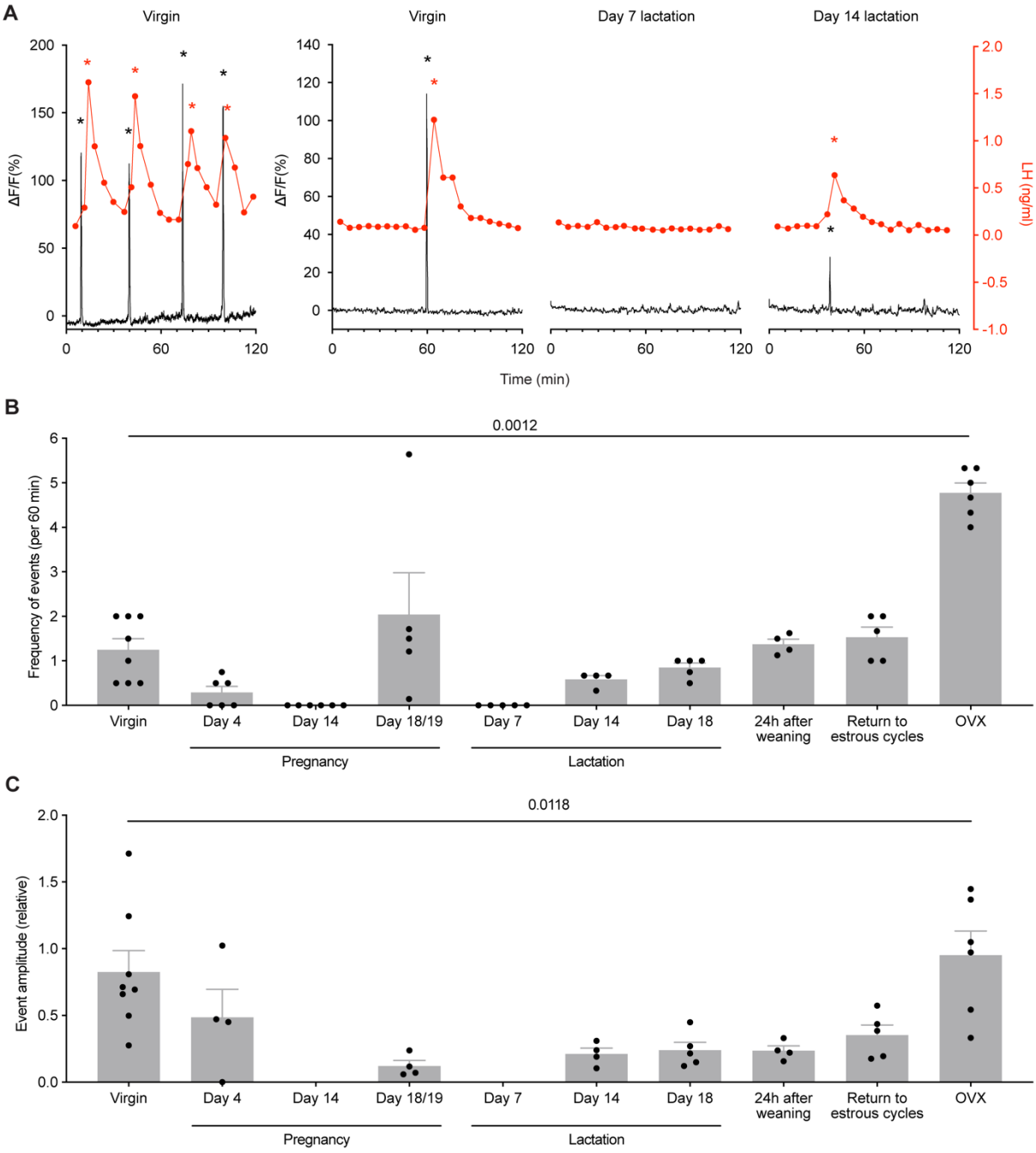

Figure 4. Synchronised Ca^{2+} events are perfectly correlated to pulsatile LH secretion across different reproductive states. (A) When fibre photometry was paired with serial blood sampling for pulsatile LH secretion, the relationship between SEs and LH pulses was examined. Each of the times an SE was seen during a recording with blood sampling, a pulse of LH was also observed, with 100% correlation ($p = <0.0001$, Chi-squared test; 73 out of 73 SEs observed lead to an LH pulse). Representative examples of paired photometry and blood sampling are shown from the diestrous state (virgin), from day 7 lactation where no SEs corresponds with no LH release, and from day 14 lactation when SE are beginning to re-

780 emerge. (B) Quantitative analysis of SE frequency per hour across different reproductive
781 states in *Kiss1*^{Cre} mice ($p = 0.0012$, mixed effect analysis (fixed type III) with Tukey's
782 multiple comparisons tests). (C) Quantitative analysis of SE amplitude of normalised $\Delta F/F$
783 across different reproductive states ($p = 0.0118$, mixed effect analysis (fixed type III) with
784 Tukey's multiple comparisons tests). Black asterisks indicate SEs, red asterisks indicate LH
785 pulse peaks as detected by PULSAR Otago analysis. Values shown as mean ± SEM.

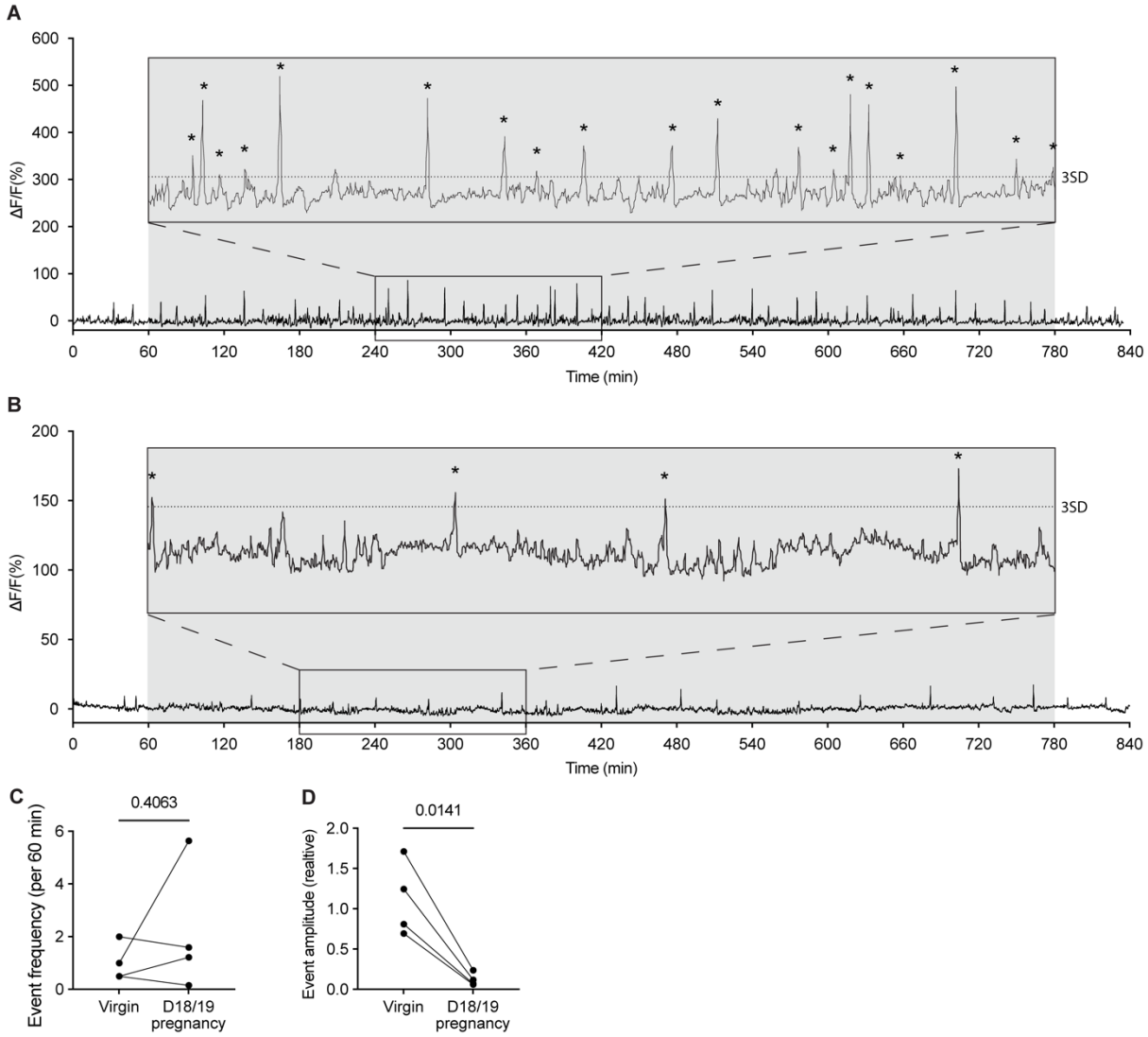

Figure 5. Activity of arcuate kisspeptin neurons on day 18/19 of pregnancy

Fibre photometry recordings of mice on the evening of day 18 of pregnancy (0600 hours) to the morning of day 19 of pregnancy day 19 (0800 hours) shows low amplitude SEs. 3-hour section blown up for ease of viewing. (C) No difference is seen between frequency of SEs (per 60 minutes) in the virgin diestrus versus D18/19 pregnancy ($p = 0.4063$, paired two-tailed t test), however a significant decrease in relative SE amplitude is seen (D; $p = 0.0141$, paired two-tailed t test). Asterisks indicate SEs. Dotted line in insert of (A) and (B) indicates 3 standard deviations (3SD). Grey shaded region = lights off.

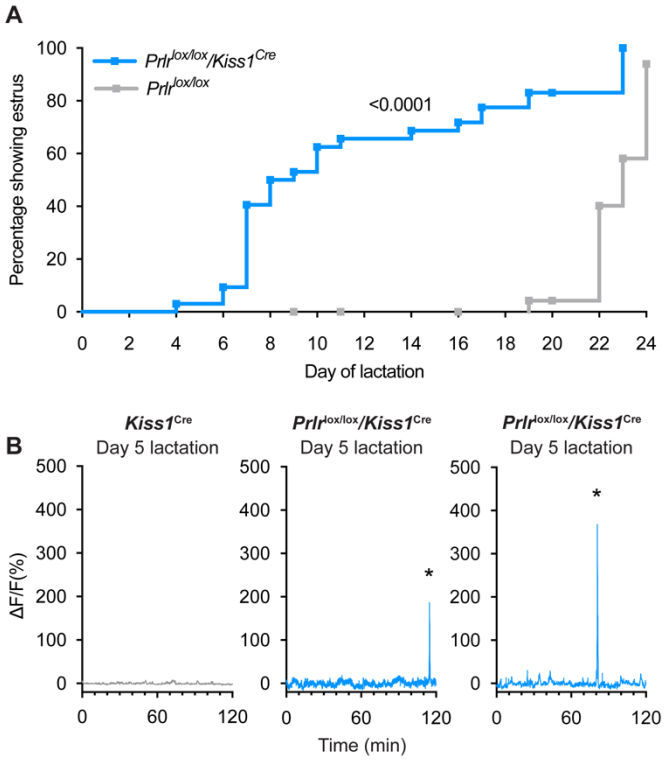

Figure 6. *Prlr*$^{lox/lox}$/*Kiss1*^{Cre} mice do not undergo the normal period of lactational infertility and show early reactivation of arcuate kisspeptin neurons prior to estrus in lactation. (A) *Prlr*$^{lox/lox}$/*Kiss1*^{Cre} mice resume estrous cycles significantly earlier (78% within 4-18 days of lactation, n = 32) than *Prlr*$^{lox/lox}$ controls (0% by day 18, n = 30) (p = <0.0001, Log-rank (Mantel-Cox) test). (B) Representative fibre photometry traces from day 5 of lactation from either a *Kiss1*^{Cre} control mouse or *Prlr*$^{lox/lox}$/*Kiss1*^{Cre} mice. Mice with Prlr knocked out of arcuate kisspeptin neurons (*Prlr*$^{lox/lox}$/*Kiss1*^{Cre}) show SEs early in lactation, which were not seen until day 14 lactation in *Kiss1*^{Cre} control mice. In comparison, the *Kiss1*^{Cre} control mouse shows no SEs, as seen in earlier groups sampled on day 7. Asterisks indicate SEs.

806 **Supplementary data**

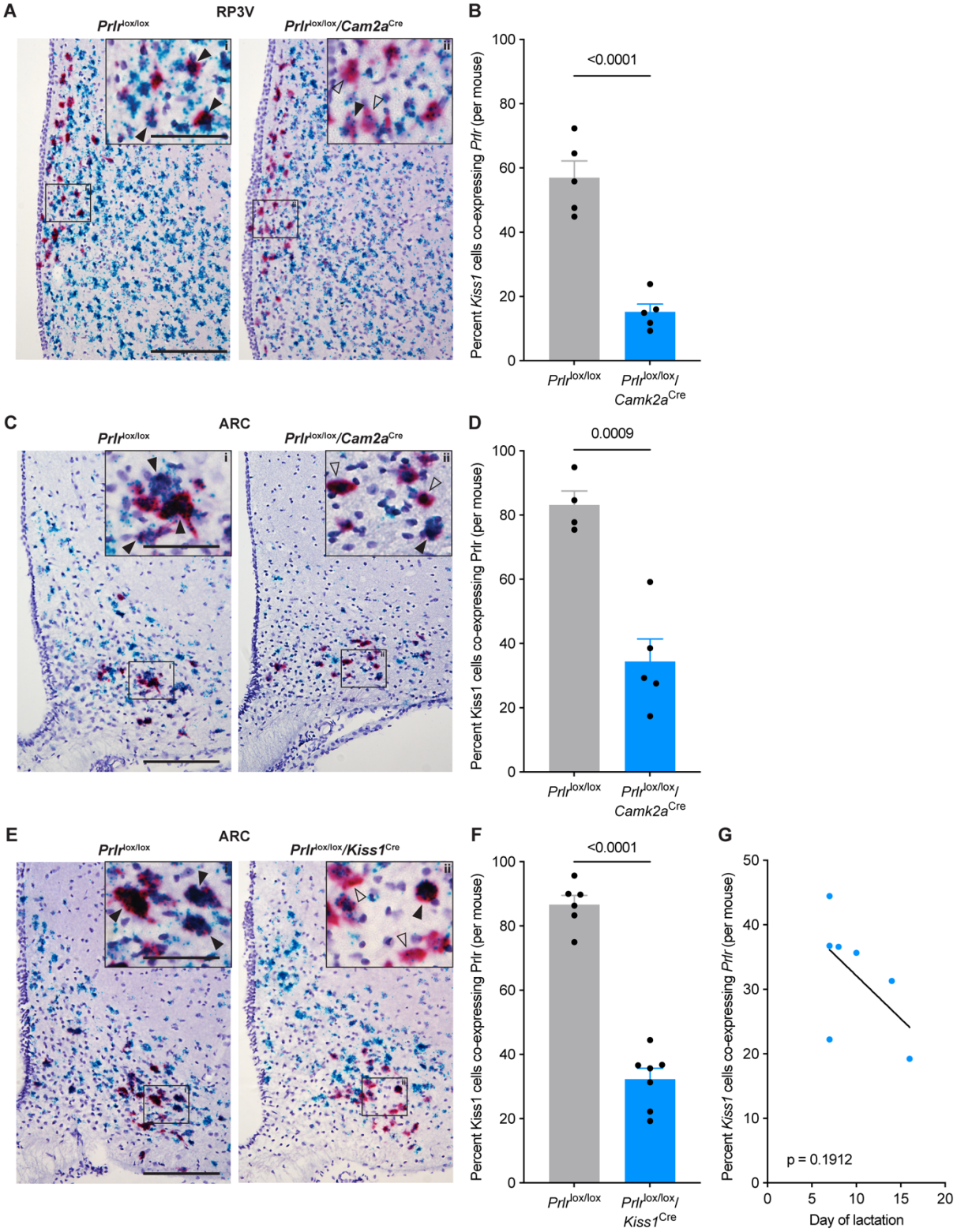

807

808

809 **Supplementary Figure 1. Proportion of kisspeptin neurons showing *Prlr* deletion using**
810 **RNAscope.** Representative photomicrographs showing RNAscope labelling for *Prlr* (blue)
811 and *Kiss1* (red) in the rostral periventricular region of the third ventricle (RP3V, A) or
812 arcuate nucleus (ARC, C, E), in either intact ($Prlr^{lox/lox}$ control n = 5, $Prlr^{lox/lox}/Camk2a^{Cre}$, n
813 = 5, A) or ovariectomised (OVX; $Prlr^{lox/lox}$ control n = 4, $Prlr^{lox/lox}/Camk2a^{Cre}$ n = 5, C;
814 $Prlr^{lox/lox}$ control n = 6, $Prlr^{lox/lox}/Kiss1^{Cre}$ n = 7, E) mice. Compared to $Prlr^{lox/lox}$ control mice,
815 $Prlr^{lox/lox}/Camk2a^{Cre}$ mice show a significant decrease in percentage of *Kiss1*-expressing cells
816 co-expressing *Prlr* in both the RP3V (B; p = <0.0001) and ARC (D; p = 0.0009) (unpaired
817 two-tailed t tests). (F) A significant decrease in the percent of *Kiss1*-expressing cells co-
818 expressing *Prlr* was seen in $Prlr^{lox/lox}/Kiss1^{Cre}$ compared to $Prlr^{lox/lox}$ controls (p = <0.0001,
819 unpaired two-tailed t test). (G) No correlation was found between percentage of *Kiss1* cells
820 co-expressing with *Prlr* and the day of estrus return during lactation (p = 0.1912, simple
821 linear regression). A *Kiss1*-expressing cell was classified as co-expressing *Prlr* mRNA if the
822 density of *Prlr* staining was above background. Solid black arrows = doubled labelled cells
823 expressing both *Kiss1* and *Prlr*; black outlined arrows = *Kiss1* cells with sparse co-labelling
824 for *Prlr*. Scale bar = 150µm, insert = 60µm. Values are shown as mean ± SEM.

825

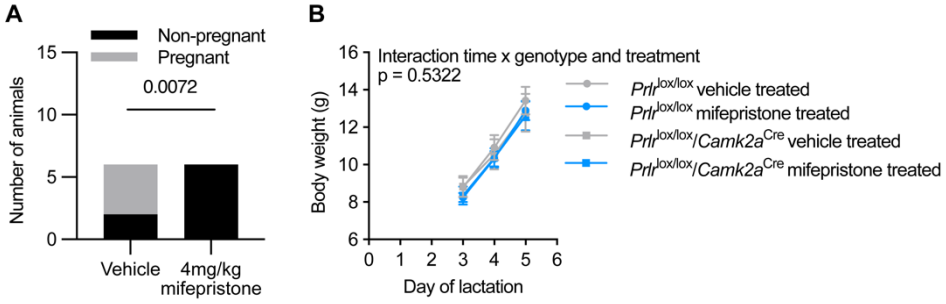

Supplementary Figure 2. Mifepristone dose response and effect on litter weight gain. (A) Mifepristone dose response trial showing dose of 4mg/kg was sufficient to terminate pregnancy in all mice ($p = 0.072$, Chi-square test, $n = 6$ both groups). (B) Mifepristone or vehicle injections had no effect on litter weight gain from day 3 to day 5 of lactation (interaction of time x genotype & treatment $p = 0.5322$; time $p = <0.0001$; genotype and treatment $p = 0.8811$; subject $p = <0.0001$; two-way ANOVA). Values are shown as mean ± SEM.

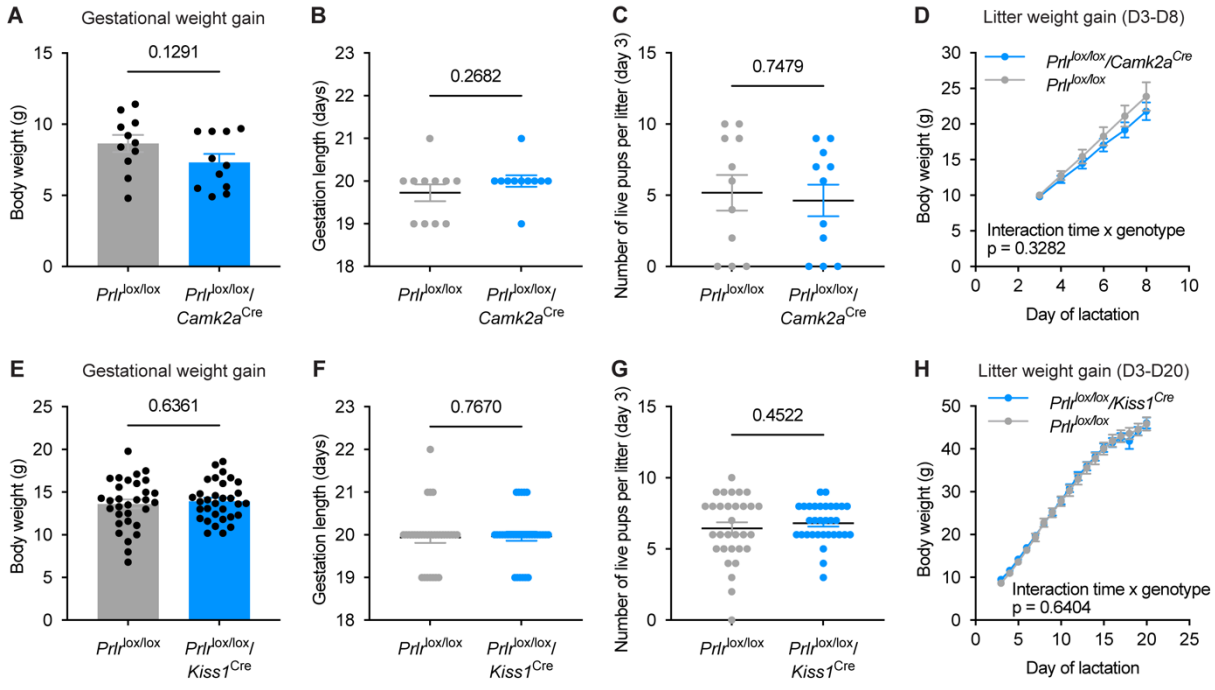

Supplementary Figure 3. Gestational and maternal phenotyping of *Prlr*$^{lox/lox}$/*Camk2a*^{Cre} and *Prlr*$^{lox/lox}$/*Kiss1*^{Cre} mice and their respective *Prlr*$^{lox/lox}$ controls. (A-H) Data show gestational weight gain (A; *Prlr*$^{lox/lox}$ n = 11, *Prlr*$^{lox/lox}$/*Camk2a*^{Cre} n = 11; E; *Prlr*$^{lox/lox}$ n = 31, *Prlr*$^{lox/lox}$/*Kiss1*^{Cre} n =27), gestation length (B; *Prlr*$^{lox/lox}$ n = 11, *Prlr*$^{lox/lox}$/*Camk2a*^{Cre} n = 11; F; *Prlr*$^{lox/lox}$ n = 31, *Prlr*$^{lox/lox}$/*Kiss1*^{Cre} n =27), number of live pups on day 3 of lactation (C; *Prlr*$^{lox/lox}$ n = 11; *Prlr*$^{lox/lox}$/*Camk2a*^{Cre} n = 11; G; *Prlr*$^{lox/lox}$ n = 31, *Prlr*$^{lox/lox}$/*Kiss1*^{Cre} n =27), and litter weight gain between day 3-8 of lactation (D; *Prlr*$^{lox/lox}$ n = 8; *Prlr*$^{lox/lox}$/*Camk2a*^{Cre} n = 8) or day 3-20 of lactation (H; *Prlr*$^{lox/lox}$ n = 22, *Prlr*$^{lox/lox}$/*Kiss1*^{Cre} n = 20). There were no differences in any of these parameters (A, C, E, G, unpaired two-tailed t test; B, F, Mann Whitney test; D, H, repeated measures mixed effect analysis, fixed effects (type III) with Šídák's multiple comparisons test. Grey = *Prlr*$^{lox/lox}$; blue A-D = *Prlr*$^{lox/lox}$/*Camk2a*^{Cre,} blue E-H = *Prlr*$^{lox/lox}$/*Kiss1*^{Cre}. Some *Prlr*$^{lox/lox}$ and *Prlr*$^{lox/lox}$/*Kiss1*^{Cre} mice were euthanised prior to day 20 lactation due to COVID-19 lockdown (*Prlr*$^{lox/lox}$ n = 5, *Prlr*$^{lox/lox}$/*Kiss1*^{Cre} n = 5), due to showing estrus and therefore euthanised 2 hours following blood sampling, or when being used as a control for one of these mice (*Prlr*$^{lox/lox}$ n =2, *Prlr*$^{lox/lox}$/*Kiss1*^{Cre} n = 2), or due to a litter losing weight (*Prlr*$^{lox/lox}$ n =1). Values are shown as mean ± SEM.

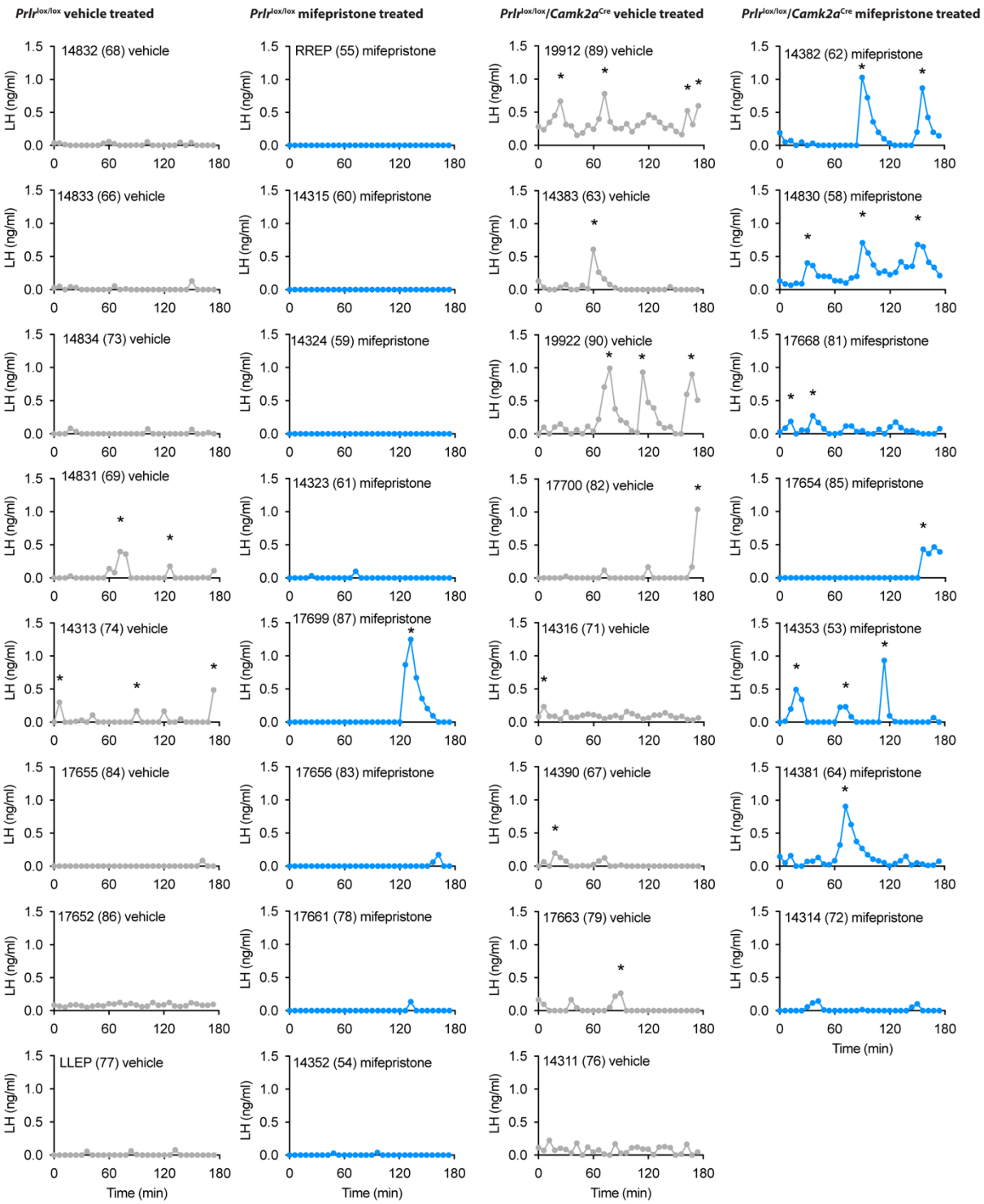
Prlr lox/lox vehicle treated
Prlr lox/lox mifepristone treated
Prlr lox/lox/Camk2a Cre vehicle treated
Prlr lox/lox/Camk2a Cre mifepristone treated
14832 (68) vehicle
RREP (55) mifepristone
19912 (89) vehicle
14382 (62) mifepristone
14833 (66) vehicle
14315 (60) mifepristone
14383 (63) vehicle
14830 (58) mifepristone
14834 (73) vehicle
14324 (59) mifepristone
19922 (90) vehicle
17668 (81) mifespristone
14831 (69) vehicle
14323 (61) mifepristone
17700 (82) vehicle
17654 (85) mifepristone
14313 (74) vehicle
17699 (87) mifepristone
14316 (71) vehicle
14353 (53) mifepristone
17655 (84) vehicle
17656 (83) mifepristone
14390 (67) vehicle
14381 (64) mifepristone
17652 (86) vehicle
17661 (78) mifepristone
17663 (79) vehicle
14314 (72) mifepristone
LLEP (77) vehicle
14352 (54) mifepristone
14311 (76) vehicle
LH (ng/ml)
Time (min)

855

856

857

858 **Supplementary Figure 4: Pulsatile LH secretion profiles of *Prlr*$^{lox/lox}$/*Camk2a*^{Cre} mice**
859 **and their controls following vehicle or mifepristone treatment.** Individual LH pulse data
860 from lactating *Prlr*$^{lox/lox}$ controls and *Prlr*$^{lox/lox}$/*Camk2a*^{Cre} mice treated with either vehicle
861 (sesame oil subcutaneous injection, grey) or 4mg/kg mifepristone (in sesame oil
862 subcutaneous injection, blue) once a day for 2 days prior to blood sampling (2 injections).
863 Lactating vehicle-treated *Prlr*$^{lox/lox}$ (n = 8), lactating mifepristone-treated *Prlr*$^{lox/lox}$ (n = 8),
864 lactating vehicle-treated *Prlr*$^{lox/lox}$/*Camk2a*^{Cre} (n = 8), lactating mifepristone-treated
865 *Prlr*$^{lox/lox}$/*Camk2a*^{Cre} (n = 7). Asterisks indicate LH pulse peaks as detected by PULSAR
866 Otago analysis.

867

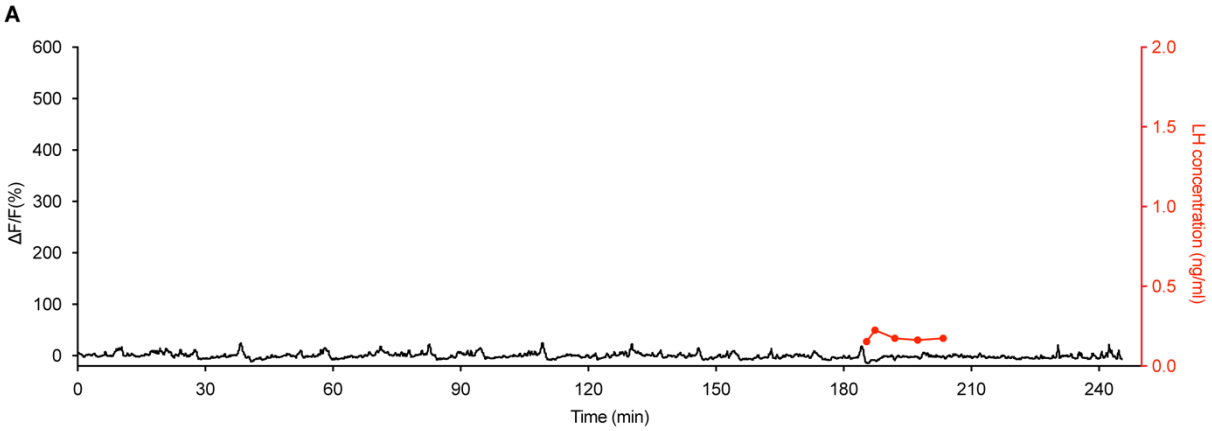

868
869 **Supplementary Figure 5. Miniature synchronised event-like activity on day 14 of**
870 **pregnancy does not result in pulsatile LH secretion.** (A) Paired fibre photometry and
871 blood sampling from mouse on day 14 of pregnancy showing miniature SE-like activity have
872 no significant effect on pulsatile LH secretion (red).

Supplementary Table 1. Statistics table. Abbreviations for tables below: DF = degrees of freedom; mc = multiple comparison; CI = 95% confidence interval; MW U = Mann Whitney U; MEA = Mixed effect analysis (fixed effects (type III)), RM = repeated measures. Ext = extended data figure.

Fig.	Description	Statistical analysis				
1C	RP3V Kisspeptin immunoreactivity in *Prlr*$^{lox/lox}$/*Camk2a*^{Cre} mice		**p**	**DF**	**CI**	**R^2**
	Interaction	Two-way ANOVA	0.0034	1		
	Genotype	Two-way ANOVA	0.0251	1		
	State	Two-way ANOVA	0.1380	1		
	Prlr$^{lox/lox}$:NL vs. *Prlr*$^{lox/lox}$:Lactating	Tukey's mc	0.0100	23	5.175 to 44.95	
	Prlr$^{lox/lox}$:NL vs. *Prlr*$^{lox/lox}$/*Camk2a*^{Cre}:NL	Tukey's mc	0.9429	23	-17.79 to 26.81	
	Prlr$^{lox/lox}$:NL vs. *Prlr*$^{lox/lox}$/*Camk2a*^{Cre}:Lactating	Tukey's mc	0.9228	23	-24.38 to 15.39	
	Prlr$^{lox/lox}$:Lactating vs. *Prlr*$^{lox/lox}$/*Camk2a*^{Cre}:NL	Tukey's mc	0.0565	23	-41.55 to 0.4412	
	Prlr$^{lox/lox}$:Lactating vs. *Prlr*$^{lox/lox}$/*Camk2a*^{Cre}:Lactating	Tukey's mc	0.0010	23	-47.97 to -11.15	
	Prlr$^{lox/lox}$/*Camk2a*^{Cre}:NL vs. *Prlr*$^{lox/lox}$/*Camk2a*^{Cre}:Lactating	Tukey's mc	0.6409	23	-30.00 to 11.99	
1D	Arcuate Kisspeptin immunoreactivity in *Prlr*$^{lox/lox}$/*Camk2a*^{Cre} mice	Unpaired two-tailed t test	0.0020	14	0.6692 to 2.424	0.5052
1E	*Prlr*$^{lox/lox}$/*Camk2a*^{Cre} do not show lactational diestrus		**p**	**X^2**	**DF**	
	Percent mice showing estrous	Log rank (Mantel-Cox) test	<0.0001	42.37	1	
2B	Effect of mifepristone treatment on LH pulse frequency in *Prlr*$^{lox/lox}$/*Camk2a*^{Cre} mice		**p**	**DF**	**CI**	
	Interaction	Two-way ANOVA	0.2807	1		
	Genotype	Two-way ANOVA	0.0024	1		
	Treatment	Two-way ANOVA	0.8558	1		
	Prlr$^{lox/lox}$:Veh vs. *Prlr*$^{lox/lox}$:Mif	Tukey's mc	0.7922	27	-0.9804 to 1.980	
	Prlr$^{lox/lox}$:Veh vs. *Prlr*$^{lox/lox}$/*Camk2a*^{Cre}:Veh	Tukey's mc	0.3861	27	-2.355 to 0.6054	
	Prlr$^{lox/lox}$:Veh vs. *Prlr*$^{lox/lox}$/*Camk2a*^{Cre}:Mif	Tukey's mc	0.1487	27	-2.765 to 0.3002	
	Prlr$^{lox/lox}$:Mif vs. *Prlr*$^{lox/lox}$/*Camk2a*^{Cre}:Veh	Tukey's mc	0.0758	27	-2.765 to 0.3002	
	Prlr$^{lox/lox}$:Mif vs. *Prlr*$^{lox/lox}$/*Camk2a*^{Cre}:Mif	Tukey's mc	0.0223	27	-2.765 to 0.3002	
	Prlr$^{lox/lox}$/*Camk2a*^{Cre}:Veh vs. *Prlr*$^{lox/lox}$/*Camk2a*^{Cre}:Mif	Tukey's mc	0.9188	27	-1.890 to 1.175	
2C	Effect of mifepristone treatment on mean LH in *Prlr*$^{lox/lox}$/*Camk2a*^{Cre} mice		**p**	**DF**		
	Interaction	Two-way ANOVA	0.8697	1		
	Genotype	Two-way ANOVA	0.0031	1		
	Treatment	Two-way ANOVA	0.8586	1		
	Prlr$^{lox/lox}$:Veh vs. *Prlr*$^{lox/lox}$:Mif	Tukey's mc	0.9947	26	-0.1021 to 0.1220	
	Prlr$^{lox/lox}$:Veh vs. *Prlr*$^{lox/lox}$/*Camk2a*^{Cre}:Veh	Tukey's mc	0.1528	26	-0.2015 to 0.02263	

Fig.	Description	Statistical analysis				
	Prlr$^{lox/lox}$:Veh vs. *Prlr*$^{lox/lox}$/*Camk2a*^{Cre}:Mif	Tukey's mc	0.1765	26	-0.2047 to 0.02672	
	Prlr$^{lox/lox}$:Mif vs. *Prlr*$^{lox/lox}$/*Camk2a*^{Cre}:Veh	Tukey's mc	0.0803	26	-0.2076 to 0.008853	
	Prlr$^{lox/lox}$:Mif vs. *Prlr*$^{lox/lox}$/*Camk2a*^{Cre}:Mif	Tukey's mc	0.0974	26	-0.2110 to 0.01306	
	Prlr$^{lox/lox}$/*Camk2a*^{Cre}:Veh vs. *Prlr*$^{lox/lox}$/*Camk2a*^{Cre}:Mif	Tukey's mc	>0.9999	26	-0.1116 to 0.1125	
4B	Kisspeptin activity across different reproductive states		**p**	**DF**	**CI**	
	Event frequency across states	MEA	0.0012			
	Virgin vs. Day 4 pregnancy	Tukey's mc	0.0828	5	-0.1356 to 2.052	
	Virgin vs. Day 14 pregnancy	Tukey's mc	0.0586	5	-0.05175 to 2.552	
	Virgin vs. Day 18/19 pregnancy	Tukey's mc	0.9837	4	-5.518 to 3.932	
	Virgin vs. Day 7 lactation	Tukey's mc	0.0912	4	-0.2517 to 2.752	
	Virgin vs. Day 14 lactation	Tukey's mc	0.6584	3	-1.598 to 2.931	
	Virgin vs. Day 18 lactation	Tukey's mc	0.9638	4	-1.661 to 2.461	
	Virgin vs. 24h after weaning	Tukey's mc	>0.9999	3	-3.097 to 2.847	
	Virgin vs. Return to estrous cycles	Tukey's mc	0.9993	4	-3.016 to 2.449	
	Virgin vs. OVX	Tukey's mc	0.0009	5	-4.955 to -2.100	
	Day 4 pregnancy vs. Day 14 pregnancy	Tukey's mc	0.5635	5	-0.3793 to 0.9626	
	Day 4 pregnancy vs. Day 18/19 pregnancy	Tukey's mc	0.6960	4	-6.958 to 3.455	
	Day 4 pregnancy vs. Day 7 lactation	Tukey's mc	0.6396	4	-0.5180 to 1.101	
	Day 4 pregnancy vs. Day 14 lactation	Tukey's mc	0.4286	3	-1.026 to 0.4430	
	Day 4 pregnancy vs. Day 18 lactation	Tukey's mc	0.2948	4	-1.579 to 0.4622	
	Day 4 pregnancy vs. 24h after weaning	Tukey's mc	0.1309	3	-2.649 to 0.4820	
	Day 4 vs. Return to estrous cycles	Tukey's mc	0.1986	4	-3.185 to 0.7012	
	Day 4 pregnancy vs. OVX	Tukey's mc	<0.0001	5	-5.683 to -3.290	
	Day 14 pregnancy vs. Day 18/19 pregnancy	Tukey's mc	0.5272	4	-7.022 to 2.936	
	Day 14 pregnancy vs. Day 7 lactation	Tukey's mc				
	Day 14 pregnancy vs. Day 14 lactation	Tukey's mc	0.0343	3	-1.092 to -0.07436	
	Day 14 pregnancy vs. Day 18 lactation	Tukey's mc	0.0092	4	-1.380 to -0.3202	
	Day 14 pregnancy vs. 24h after weaning	Tukey's mc	0.0072	3	-2.072 to -0.6781	
	Day 14 pregnancy vs. Return to estrous cycles	Tukey's mc	0.0210	4	-2.731 to -0.3355	
	Day 14 pregnancy vs. OVX	Tukey's mc	<0.0001	5	-5.877 to -3.679	
	Day 18/19 pregnancy vs. Day 7 lactation	Tukey's mc	0.6053	3	-4.432 to 8.518	
	Day 18/19 pregnancy vs. Day 14 lactation	Tukey's mc	0.9434	2	-11.74 to 14.66	
	Day 18/19 pregnancy vs. Day 18 lactation	Tukey's mc	0.9458	3	-5.853 to 8.239	
	Day 18/19 pregnancy vs. 24h after weaning	Tukey's mc	0.9807	2	-6.951 to 8.287	
	Day 18/19 pregnancy vs. Return to estrous cycles	Tukey's mc	0.9952	3	-4.164 to 5.183	
	Day 18/19 pregnancy vs. OVX	Tukey's mc	0.2556	4	-7.450 to 1.980	
	Day 7 lactation vs. Day 14 lactation	Tukey's mc	0.0382	3	-1.112 to -0.05439	
	Day 7 lactation vs. Day 18 lactation	Tukey's mc	0.0325	3	-1.578 to -0.1222	
	Day 7 lactation vs. 24h after weaning	Tukey's mc	0.0412	2	-2.620 to -0.1304	
	Day 7 lactation vs. Return to estrous cycles	Tukey's mc	0.0514	3	-3.083 to 0.01609	
	Day 7 lactation vs. OVX	Tukey's mc	0.0002	4	-5.887 to -3.669	

Fig.	Description	Statistical analysis				
	Day 14 lactation vs. Day 18 lactation	Tukey's mc	0.8130	3	-1.405 to 0.8715	
	Day 14 lactation vs. 24h after weaning	Tukey's mc	0.1642	2	-2.285 to 0.7020	
	Day 14 lactation vs. Return to estrous cycles	Tukey's mc	0.2736	2	-3.366 to 1.466	
	Day 14 lactation vs. OVX	Tukey's mc	0.0026	3	-5.734 to -2.655	
	Day 18 lactation vs. 24h after weaning	Tukey's mc	0.1662	3	-1.362 to 0.3122	
	Day 18 lactation vs. Return to estrous cycles	Tukey's mc	0.1946	3	-1.849 to 0.4823	
	Day 18 lactation vs. OVX	Tukey's mc	0.0016	4	-5.475 to -2.380	
	24h after weaning vs. Return to estrous cycles	Tukey's mc	0.9643	3	-1.180 to 0.8630	
	24h after weaning vs. OVX	Tukey's mc	0.0080	3	-5.192 to -1.614	
	Return to estrous cycles vs OVX	Tukey's mc	0.0113	4	-5.382 to -1.107	
4C	Kisspeptin activity across different reproductive states		**p**	**DF**	**CI**	
	Event amplitude across states	MEA	0.0118			
	Virgin vs. Day 4	Tukey's mc	0.7336	3	-0.9745 to 1.654	
	Virgin vs. Day 18/19	Tukey's mc	0.2608	3	-0.6762 to 2.086	
	Virgin vs. Day 14	Tukey's mc	0.0851	3	-0.1362 to 1.365	
	Virgin vs. Day 18	Tukey's mc	0.1766	4	-0.2966 to 1.467	
	Virgin vs. 24h after weaning	Tukey's mc	0.4700	3	-0.9997 to 2.178	
	Virgin vs. Return to estrous cycles	Tukey's mc	0.4514	4	-0.5997 to 1.546	
	Virgin vs. OVX	Tukey's mc	0.9938	5	-0.9886 to 0.7359	
	Day 4 vs. Day 18/19	Tukey's mc	0.7336	1	-5.882 to 6.612	
	Day 4 vs. Day 14	Tukey's mc	0.7858	2	-1.431 to 1.981	
	Day 4 vs. Day 18	Tukey's mc	0.6250	2	-0.9138 to 1.405	
	Day 4 vs. 24h after weaning	Tukey's mc	0.2399	1	-0.8660 to 1.365	
	Day 4 vs. Return to estrous cycles	Tukey's mc	0.9217	2	-1.026 to 1.293	
	Day 4 vs. OVX	Tukey's mc	0.5530	3	-1.870 to 0.9381	
	Day 18/19 vs. Day 14	Tukey's mc	0.7069	2	-0.5763 to 0.3960	
	Day 18/19 vs. Day 18	Tukey's mc	0.1985	3	-0.3267 to 0.08725	
	Day 18/19 vs. 24h after weaning	Tukey's mc	0.6222	2	-0.6603 to 0.4286	
	Day 18/19 vs. Return to estrous cycles	Tukey's mc	0.2384	2	-0.7754 to 0.3120	
	Day 18/19 vs. OVX	Tukey's mc	0.1494	3	-2.103 to 0.4405	
	Day 14 vs. Day 18	Tukey's mc	0.9929	3	-0.3118 to 0.2526	
	Day 14 vs. 24h after weaning	Tukey's mc	0.5747	2	-0.1375 to 0.08624	
	Day 14 vs. Return to estrous cycles	Tukey's mc	0.4210	2	-0.6226 to 0.3396	
	Day 14 vs. OVX	Tukey's mc	0.3306	3	-2.375 to 0.8931	
	Day 18 vs. 24h after weaning	Tukey's mc	>0.9999	3	-0.3977 to 0.4056	
	Day 18 vs. Return to estrous cycles	Tukey's mc	0.6644	3	-0.5038 to 0.2799	
	Day 18 vs. OVX	Tukey's mc	0.1809	4	-1.793 to 0.3702	
	24h after weaning vs. Return to estrous cycles		0.5101	3	-0.4457 to 0.2140	
	24h after weaning vs. OVX	Tukey's mc	0.2874	3	-2.185 to 0.7540	
	Return to estrous cycles vs. OVX	Tukey's mc	0.2096	4	-1.563 to 0.3637	
5C	Virgin vs day 18/19 pregnancy frequency of events		**p**	**R^2**	**CI**	
		Paired two-tailed t test	0.4063	0.2364	-2.646 to 4.945	
5D	Virgin vs day 18/19 pregnancy relative event amplitude		**p**	**R^2**	**CI**	
		Paired two-tailed t test	0.0141	0.8989	-1.606 to -0.3816	
6A	*Prlr*$^{lox/lox}$/*Kiss1*^{Cre} do not show lactational diestrus		**p**	**X^2**	**DF**	
	Percent mice showing estrus	Log rank (Mantel-Cox) test	<0.0001	38.02	1	
Ext 1A-D	*Prlr*$^{lox/lox}$/*Camk2a*^{Cre} maternal and gestational phenotyping		**p**	**R^2**	**CI**	**MW U**
	A: gestational weight gain	Unpaired two-tailed t test	0.1291	0.1113	-3.076 to 0.4219	
	B: gestation length	Mann Whitney test	0.2682			45.50

Fig.	Description	Statistical analysis				
	C: number of live pups	Unpaired two-tailed t test	0.7479	0.005282	-4.037 to 2.946	
	D: litter weight gain					
	Time	MEA	<0.0001			
	Genotype	MEA	0.3833			
	Time x genotype	MEA	0.3282			
	Day 3 lactation	Šídák's mc	>0.9999		-3.740 to 4.115	
	Day 4 lactation	Šídák's mc	0.9993		-3.365 to 4.490	
	Day 5 lactation	Šídák's mc	0.9863		-2.965 to 4.890	
	Day 6 lactation	Šídák's mc	0.9525		-2.690 to 5.165	
	Day 7 lactation	Šídák's mc	0.6938		-1.953 to 5.903	
	Day 8 lactation	Šídák's mc	0.619		-1.821 to 6.112	
Ext1 E-H	*Prlr*$^{lox/lox}$/*Kiss1*^{Cre} maternal and gestational phenotyping		**p**	**R^2**	**CI**	**MW U**
	E: gestational weight gain	Unpaired two-tailed t test	0.6361	0.003694	-0.9985 to 1.622	
	F: gestation length	Mann Whitney test	0.7670			471.5
	G: number of live pups	Unpaired two-tailed t test	0.4522	0.009296	-0.5930 to 1.315	
	H: litter weight gain					
	Time x Genotype	Two-way RM ANOVA	0.6404			
	Time	Two-way RM ANOVA	<0.0001			
	Genotype	Two-way RM ANOVA	0.9014			
	Subject	Two-way RM ANOVA	<0.0001			
	Day 3 lactation	Šídák's mc	>0.9999		-5.407 to 3.653	
	Day 4 lactation	Šídák's mc	>0.9999		-5.204 to 3.857	
	Day 5 lactation	Šídák's mc	>0.9999		-5.159 to 3.902	
	Day 6 lactation	Šídák's mc	>0.9999		-5.105 to 3.956	
	Day 7 lactation	Šídák's mc	>0.9999		-4.976 to 4.084	
	Day 8 lactation	Šídák's mc	>0.9999		-4.226 to 4.834	
	Day 9 lactation	Šídák's mc	>0.9999		-4.757 to 4.304	
	Day 10 lactation	Šídák's mc	>0.9999		-4.650 to 4.410	
	Day 11 lactation	Šídák's mc	>0.9999		-5.154 to 3.907	
	Day 12 lactation	Šídák's mc	>0.9999		-5.242 to 3.819	
	Day 13 lactation	Šídák's mc	>0.9999		-4.936 to 4.125	
	Day 14 lactation	Šídák's mc	>0.9999		-4.979 to 4.081	
	Day 15 lactation	Šídák's mc	>0.9999		-4.776 to 4.284	
	Day 16 lactation	Šídák's mc	>0.9999		-4.152 to 4.909	
	Day 17 lactation	Šídák's mc	>0.9999		-4.216 to 4.845	
	Day 18 lactation	Šídák's mc	0.9912		-2.717 to 6.343	
	Day 19 lactation	Šídák's mc	>0.9999		-4.182 to 4.878	
	Day 20 lactation	Šídák's mc	>0.9999		-4.752 to 4.309	
Ext 3	Proportion of kisspeptin neurons showing *Prlr* deletion using RNAscope		**p**	**R^2**	**CI**	
	B: *Prlr*$^{lox/lox}$/*Camk2a*^{Cre} RP3V	Unpaired two-tailed t test	<0.0001	0.8740	-55.02 to 28.69	
	D: *Prlr*$^{lox/lox}$/*Camk2a*^{Cre} ARC	Unpaired two-tailed t test	0.0009	0.8123	-69.72 to 8.860	
	F: *Prlr*$^{lox/lox}$/*Kiss1*^{Cre} ARC	Unpaired two-tailed t test	<0.0001	0.9300	-64.27 to -44.46	
	G: correlation of day of estrus and average density of *Prlr* on *Kiss1*-expressing cells (per animal)	Simple linear regression	0.1912	0.3135		
Ext 4A	Mifepristone functional dose response trial		**p**	**X^2**	**Z**	
		Chi-square test	0.0072	6	2.449	
Ext 4B	Mifepristone has no effect on litter weight gain		**p**	**DF**		
	Time x Genotype and treatment	Two-way RM ANOVA	0.5322	6		
	Time	Two-way RM ANOVA	<0.0001	2		
	Genotype and treatment	Two-way RM ANOVA	0.8811	3		

Fig.	Description	Statistical analysis				
	Subject	Two-way RM ANOVA	<0.0001	22		